

ARTICLE OPEN



Taurine as a key intermediate for host-symbiont interaction in the tropical sponge *Ianthella basta*

Florian U. Moeller¹, Craig W. Herbold¹, Arno Schintlmeister^{1,2}, Maria Mooshammer¹, Cherie Motti³, Bettina Glasl¹, Katharina Kitzinger¹, Faris Behnam¹, Margarete Watzka⁴, Thomas Schweder^{1,5,6}, Mads Albertsen^{1,7}, Andreas Richter^{1,4}, Nicole S. Webster^{3,8,9} and Michael Wagner^{1,2,7}✉

© The Author(s) 2023

Marine sponges are critical components of marine benthic fauna assemblages, where their filter-feeding and reef-building capabilities provide benthic-pelagic coupling and crucial habitat. As potentially the oldest representation of a metazoan-microbe symbiosis, they also harbor dense, diverse, and species-specific communities of microbes, which are increasingly recognized for their contributions to dissolved organic matter (DOM) processing. Recent omics-based studies of marine sponge microbiomes have proposed numerous pathways of dissolved metabolite exchange between the host and symbionts within the context of the surrounding environment, but few studies have sought to experimentally interrogate these pathways. By using a combination of metaproteogenomics and laboratory incubations coupled with isotope-based functional assays, we showed that the dominant gammaproteobacterial symbiont, ‘*Candidatus Taurinisymbion ianthellae*’, residing in the marine sponge, *Ianthella basta*, expresses a pathway for the import and dissimilation of taurine, a ubiquitously occurring sulfonate metabolite in marine sponges. ‘*Candidatus Taurinisymbion ianthellae*’ incorporates taurine-derived carbon and nitrogen while, at the same time, oxidizing the dissimilated sulfite into sulfate for export. Furthermore, we found that taurine-derived ammonia is exported by the symbiont for immediate oxidation by the dominant ammonia-oxidizing thaumarchaeal symbiont, ‘*Candidatus Nitrosospongia ianthellae*’. Metaproteogenomic analyses also suggest that ‘*Candidatus Taurinisymbion ianthellae*’ imports DMSP and possesses both pathways for DMSP demethylation and cleavage, enabling it to use this compound as a carbon and sulfur source for biomass, as well as for energy conservation. These results highlight the important role of biogenic sulfur compounds in the interplay between *Ianthella basta* and its microbial symbionts.

The ISME Journal (2023) 17:1208–1223; <https://doi.org/10.1038/s41396-023-01420-1>

INTRODUCTION

Marine sponges are important components of coral reefs with a range of critical ecological functions [1]. Sponges play a crucial role in maintaining biomass in reef ecosystems by filtering dissolved organic matter (DOM) from large quantities of water and capturing it as biomass, which is then shed as particulate organic matter (POM) and passed to higher trophic levels [2–4]. Marine sponges often harbor dense, diverse, and stable communities of microorganisms that are thought to play a role in DOM processing, as well as a broad suite of other nutrient transformations [3, 5, 6]. These microbial symbionts have been shown to photosynthetically fix carbon [7], fix N₂ [8], nitrify [9, 10], as well as carry out anammox, denitrification, and sulfate respiration [11, 12]. Furthermore, isotope labeling experiments have proven that symbiont-derived carbon and nitrogen can be found in sponge cells [7, 11, 13, 14], with more recent studies revealing an emerging view that not only microbial symbionts can incorporate

DOM, but that sponge cells do as well, and can even translocate DOM-derived carbon and nitrogen to their symbionts [15–17].

Whilst the specificity, biogeography, and environmental sensitivity of the relationship between sponges and their microbiome has been intensively studied [18–20], our understanding of the physiological interactions between sponges and their symbiotic microorganisms is still very limited. Genome-based investigations of the sponge microbiome have revealed an array of diverse metabolic potential encoded in symbiont genomes, including the processing of organic carbon, nitrogen, and sulfur compounds [21–24], autotrophic sulfur oxidation [25, 26], and vitamin synthesis [27, 28]. These metabolic processes may be mediated by a diverse array of transporters, encoded in the symbionts, to facilitate exchange with the host, as well as the surrounding environment (reviewed in [29]). In a few studies, metaproteomic analyses have revealed the expression of proteins indicative of metabolic interactions between the host and symbionts, including

¹Centre for Microbiology and Environmental Systems Science, Division of Microbial Ecology, University of Vienna, Vienna, Austria. ²Large-Instrument Facility for Environmental and Isotope Mass Spectrometry, Centre for Microbiology and Environmental Systems Science, University of Vienna, Vienna, Austria. ³Australian Institute of Marine Science, Townsville, QLD, Australia. ⁴Centre for Microbiology and Environmental Systems Science, Division of Terrestrial Ecosystem Research, University of Vienna, Vienna, Austria. ⁵Institute of Marine Biotechnology e.V., Greifswald, Germany. ⁶Institute of Pharmacy, Pharmaceutical Biotechnology, University of Greifswald, Greifswald, Germany. ⁷Center for Microbial Communities, Department of Chemistry and Bioscience, Aalborg University, Aalborg, Denmark. ⁸Australian Centre for Ecogenomics, School of Chemistry and Molecular Biosciences, University of Queensland, St Lucia, St Lucia, QLD, Australia. ⁹Australian Antarctic Division, Kingston, TAS, Australia. ✉email: michael.wagner@univie.ac.at

Received: 23 September 2022 Revised: 14 April 2023 Accepted: 20 April 2023

Published online: 15 May 2023

transport functions for typical sponge metabolites, and the potential mediation of host-symbiont interactions via the expression of eukaryotic-like proteins and cell-cell mediators [10, 30]. Despite these insights obtained from a variety of approaches, the high complexity of sponge holobionts, coupled with the inherent difficulty in culturing sponge symbionts, has made it challenging to irrevocably link host interactions and symbiont physiology with symbiont phylogeny.

One way of examining host-symbiont interaction, is by tracking compounds that may be translocated from the host to the symbiont, such as taurine. Taurine has been reported from a broad suite of sponge species, oftentimes as one of the most abundant free amino acids (up to 39% of the free amino acid pool; [31]). Free-living marine bacteria can utilize taurine produced by phytoplankton [32–34] and the genetic capacity for taurine utilization has been identified in many marine sponge microbiomes [25, 26, 35–37]. Taurine has been proposed to be an important intermediate driving metabolic exchange between marine bacteria and eukaryotic phytoplankton [32–34, 38], and yet, to date, there is no direct experimental evidence for the utilization of host-derived taurine by marine symbionts, and of its role in mediating holobiont function, despite the abundance and widespread distribution of this compound in marine animals. However, taurine has recently been demonstrated to confer resistance to pathogens in mammalian gut systems, wherein taurine-metabolizing gut microbiota shield the host against infections, by converting taurine to sulfide, an inhibitor of cellular respiration [39, 40]. Taurine is an ideal osmoregulator, as it is transported by a Na⁺-dependent transport system unique to β-amino acids and so, it is responsive to ionic activities and other osmotic agents [41, 42]. As a zwitterionic compound, extremely high intra- to extracellular concentration gradients for taurine can be maintained, and due to its lipophobic properties, it is not readily lost by diffusion [43]. Taurine also likely functions as a storage and transport compound, providing nitrogen and sulfur to symbionts in the gutless clams *Solemya reidi* [44] and *Solemya velum* [45]. The synthesis of sulfur-containing free amino acids has long been proposed as a strategy for sulfide detoxification and transport in chemoautotrophic symbioses [46–50] and taurine is the dominant free amino acid in many of these species [44, 46–50].

Ianthella basta [51] is a widely distributed sponge species found throughout the Indo-Pacific region [52]. In contrast to many marine sponge species with high microbial abundance of microbial symbionts [53], *I. basta* hosts only a low diversity of microbial symbionts and is populated by three dominant phylotypes including an alphaproteobacterium, a gammaproteobacterium and a thaumarchaeote, which all occur at relatively high abundances in the sponge mesohyl [10, 54, 55]. This “low complexity” community is highly stable across different host morphotypes [56], across the large geographic range of the host, under different host health states [55], and across a wide suite of environmental conditions [57]. Thus, the *I. basta* holobiont represents a comparatively tractable model system for the investigation of sponge-symbiont physiological interactions. Recently, we were able to demonstrate that the thaumarchaeal symbiont of *I. basta* — ‘*Candidatus Nitrosospongia ianthellae*’ — is an active ammonia oxidizer and that, surprisingly, this sponge does not harbor a bacterial nitrite oxidizer [10]. However, the physiology of the remaining two symbiont phylotypes remains unknown. In this study, we elucidate selected physiological traits of the metagenome-assembled genome (MAG) of this symbiont, we focused on the important biogenic sulfonate intermediate, taurine. We document the expression of a previously described [58], but infrequently observed pathway for the transport and dissimilation of taurine into sulfite, followed by sulfite oxidation into sulfate, encoded by the symbiont, and provide experimental physiological support for this sponge-microbe interaction. For this purpose, we

performed whole sponge incubations with added taurine and detected the predicted secreted end product, sulfate. We also employed the use of stable isotope-labeled taurine to track the incorporation of taurine-derived carbon and nitrogen into *I. basta* holobiont biomass, as well as the dissimilation of the nitrogen moiety to ammonium and its subsequent oxidation to nitrite.

MATERIALS AND METHODS

Sponge collection for metaproteogenomics and *Ianthella basta* holobiont taurine incubations

Two specimens of the purple thick morphotype of the sponge *Ianthella basta* were collected in waters offshore from Orpheus Island (18°36.878'S, 146°29.990'E), Queensland, Australia, in October 2010 and 2011, and processed as described in [10] for metaproteogenomic analysis. In addition, sponge explants were used for 48-h batch incubations, either in the presence or absence of taurine. The sponge explants used for the taurine incubations were derived from two large yellow thin morph *Ianthella basta* individuals (approx. 0.5 m × 0.5 m × 0.5 cm) collected from Davies Reef (18°49.354 S, 147°38.253 E) on 21st November 2014 and 25th August 2015. Upon collection, the individuals were maintained in flow-through reef seawater onboard the RV Cape Ferguson until their return to the Australian Institute of Marine Science (AIMS) where the individuals were cut into small sponge explants between 10 × 10 × 0.5 cm and 5 × 5 × 0.5 cm and left to heal in aquaria overnight. Since *I. basta* individuals are thin, erect, and laminar, while also exhibiting incurrent (ostia) and excurrent holes (oscula) that are spaced approximately 1 cm apart and on opposing sides of the sponge, relatively small samples can be representative of the entire aquiferous system [59]. The explants were prepared by cutting rectangular-like shapes, while preserving both sides of the fan-shaped sponge, thereby retaining multiple oscula and ostia on both sides. All explants were monitored at the beginning and end of the incubations for tissue health, and no major signs of tissue health regression or necrosis were observed. Furthermore, the edges of the cut sides are estimated to represent 4–8% of the volume of each explant (by assuming an edge thickness of 0.1 cm) and thus, the area of tissue wounds are small relative to the size of each explant. Live sponge explants were transferred to sulfate-free artificial seawater (SFASW; see Supplementary Note for media details) and rinsed three times to remove as much sulfate from seawater as possible. For all incubation experiments, *I. basta* explants were incubated at 25 °C in the dark, in continuously stirred acid-washed glass tanks, either filled with 0.2 μm natural filtered seawater (FSW) or SFASW, and with or without taurine added at different time points and concentrations. All incubations were conducted in the dark to preclude light inhibition of nitrification. SFASW incubations were conducted to more readily discern the production of sulfate from the taurine-dissimilation/sulfite oxidation pathway, since natural seawater contains sulfate at high concentrations. In the first set of experiments, 1 mM unlabeled taurine was added at the beginning of the incubations and another 0.6 mM pulse was added at t = 36 h. For stable isotope incubations in standard seawater, ¹⁵N and ¹³C labeled taurine (2-Amino-¹⁵N-ethanesulfonic acid: Taurine-¹⁵N, 98 atom%; 2-Aminoethane-¹³C2-sulfonic Acid: Taurine-¹³C2, 99 atom%; Campro Scientific GmbH, Berlin, Germany) were added in equimolar concentrations (i.e., a total of 0.8 mM of ¹⁵N-taurine and 0.8 mM of ¹³C-taurine were added by the end of the incubations) simultaneously, so as to monitor potential incorporation into *I. basta* holobiont biomass, as well as to track dissimilation into NH₄⁺, followed by successive oxidation to NO₂⁻ by the dominant thaumarchaeal symbiont [10]. For these two sets of experiments, incubations were conducted in closed 1 l acid-washed glass aquaria at room temperature and water sampling occurred at t = 0, 12, and 48 h, while sampling of *I. basta* biological material occurred at the end of the experiment at t = 48 h. These two experiments utilized 12 explants (approx. 10 × 10 × 0.5 cm; 9.14 ± 2.4 g sponge wet weight) from the individual collected in November 2014 (3 replicates per treatment with *I. basta* explants: SFASW + *I. basta*; SFASW + taurine + *I. basta*; FSW + *I. basta*; FSW + ¹³C¹⁵N-labeled taurine + *I. basta*). An additional follow-up experiment was conducted with explants derived from the individual collected in October 2015, in SFASW in closed 250 ml acid-washed glass aquaria but with higher temporal resolution (t = 0, 12, 24, 36, and 48 h), and 1 mM or 100 μM isotopically unlabeled taurine added at the beginning of the incubation. This set of experiments utilized 45 explants (approx. 5 × 5 × 0.5 cm; 2.98 ± 0.82 g sponge wet wt), as each explant was sacrificially sampled at the end of each time point. For all sets of incubations, parallel control incubations were performed under identical

conditions, but without *I. basta* explants. All incubations were conducted in triplicates. We treated the explants from the same *I. basta* individual as non-technical replicates, since differences in symbiont distribution within the relatively large sponge individuals used here, may occur.

For chemical analyses, seawater samples (10 ml) were taken from the containers (see above-described set of experiments) and filtered using 0.45 µm Sartorius Minisart cellulose acetate filters (Göttingen, Germany). Duplicate samples for dissolved inorganic nitrogen (NH_4^+ , NO_2^- , NO_3^-) were measured on a Seal AA3 segmented flow analyser and referenced against OSIL standards and in-house reference samples. Sulfate was measured via ion chromatography, followed by detection via suppressed conductivity. Confirmation of taurine uptake by *I. basta* was established following an adapted two-step pre-column fluorometric derivatization HPLC method [60]. O-phthalaldehyde-ethanethiol (OPA-ET; Sigma Aldrich; 750 µl), prepared daily in methanol (MeOH; Sharlau), buffered with 0.8 M borate (Sigma Aldrich; pH 11), and aged at 4 °C for 2 h, was added to 100 µl of seawater sample diluted in 900 µl MilliQ H₂O. After 1 min, 50 µl of fluorenylmethylxycarbonyl chloride (FMOC-Cl) [Sigma Aldrich], prepared in acetonitrile [Sharlau], and aged for at least 12 h, was added; the higher concentration of the derivatizing reagents was required to ensure complete reaction of the taurine (~mM). After a further 1 min, 10 µl of the derivatized sample was injected onto an Agilent 1100 HPLC system (comprising a binary pump, autosampler, column oven, and fluorescence detector, and operated using Chemstation for LC 3D Rev. A.10.01 and 735 Sampler Software v6.10). Samples ($n = 2$ samples per treatment per timepoint; $n = 5$ replicate injections per sample) were chromatographed on a 250 × 4.6 mm i.d., 5 µm particle size, HILIC (Phenomenex) column under the following conditions: 1 ml min⁻¹ flow rate; column maintained at 40 °C; mobile phases comprising MeOH-sodium acetate (0.36 M; pH 7.0)-H₂O (55:8:37, v/v/v) (A) and acetonitrile-sodium acetate (0.36 M; pH 7.0)-H₂O (10:5:85, v/v/v) (B); gradient 15% A at 0–2 min, 15–20% A at 2–6 min, 40% A at 6–9 min, 85% A at 9–17 min then held until 20 min; the column was flushed with 100% A at 20–21 min and held for a further 4 min before re-equilibration at 15% A for 5 min; fluorescence detection (excitation: 330 nm, emission: 460 nm). For calibration, a taurine stock solution (1 M; > 99.9% Sigma Aldrich) was prepared in Milli-Q water and a dilution series prepared (10 mM–1 nM). γ-Aminobutyric acid (5 M GABA; Sigma Aldrich) was used as the internal standard. The dilution series was stored at 4 °C. The calibration curve ($R^2 = 0.99$) was used to quantify taurine in seawater. ¹⁵N-analyses of ammonium and nitrite from the incubation experiments with stable-isotope labeled taurine are described below.

Metagenome assembly and genome binning

Sequencing libraries were prepared from the same DNA extracted from the individual collected in October 2010 [10] using the Nextera kit (Illumina) according to the manufacturer's instructions and concentrations measured using the QuantIT kit (Molecular Probes, Life Technologies, Naerum, Denmark). The libraries were paired-end (2 × 150 bp) sequenced on an HiSeq 2000 System (Illumina) using the TruSeq PE Cluster Kit v3-cBot-HS and TruSeq SBS kit v.3-HS sequencing kit, and on an Illumina MiSeq using v3 sequencing kits (2 × 300 bp). Metagenome reads in fastq format, obtained from the sequencing runs, were end-trimmed at a minimum phred score of 15, a minimum length of 50 bp, allowing no ambiguous nucleotides, and sequencing adaptors removed. Trimmed reads from each dataset were assembled using SPAdes version 3.11.0 [61], using default parameters, and genomes were binned using Metabat v 2.12.0 [62]. The choice of SPAdes was made as previous analyses [10] showed that SPAdes returned higher quality MAGs on average for both the archaeal and gammaproteobacterial symbionts. MAGs from multiple Illumina datasets were dereplicated using dRep [63] and provisionally classified using CheckM [64]. A single high-quality gammaproteobacterial MAG was recovered after dereplication and uploaded to MaGe [65] for annotation. The mapped read pairs (at >98% identity) for the assembly of this MAG represented 3.02% of total QC paired reads and read coverage was approximately 26X.

Two additional MAGs were assembled and binned from paired end reads from SRA runs derived from two sponge species, belonging to the same family as *Ianthella basta* (*Hexadella deditifera* and *Hexadella cf. deditifera*) [66]. Paired end reads for SRA runs SRR8088660, SRR8088661, SRR8088662, and SRR8088663 were downloaded from NCBI. BBduk (bbmap v37.61) was used to remove adapters and residual phiX (adapters.fa, phix174_ill.ref.fa.gz, ktrim = r k = 21 mink = 11 hdist = 2), then quality filtered (minlen = 99 qtrim = r trimq = 15). Read sets were denoised using BayesHammer (SPAdes v3.15.3) [61] and merged using

bbmerge (bbmap v37.61). Reads were assembled using SPAdes v3.15.3 (-k 21,33,55,77 --only-assemble) and metaSPAdes (-k 21,33,55,77 --only-assemble) resulting in 8 assemblies (2 assemblers, 4 datasets). Each read set was mapped against each assembly using bbmap v37.61 (minid = 0.99 idfilter = 0.99 ambiguous = best pairedonly = t killbadpairs = t mappedonly = t) and MAGs were generated using metabat1 and metabat2 algorithms (metabat v2.15). MAGs from each SRA run were then dereplicated with dRep v1.4.3 dereplicate_wf (-comp 40 -con 10 -l 200000) [63]. "Winning" MAGs from each SRA run were combined and dereplicated using dRep v1.4.3 (-comp 40 -con 10 -l 200000 -pa 0.6 --S_algorithm gANI --S_ani 0.965). Reads from each SRA run were remapped to each MAG using bbmap v37.61 (minid = 0.99 idfilter = 0.99 ambiguous = best pairedonly = t killbadpairs = t mappedonly = t) and relative abundance was calculated, by dividing mapped fragments by total fragments, for each metagenomic dataset.

Cryosectioning and FISH for relative symbiont quantification

The aforementioned *I. basta* individual, collected for metagenomic sequencing in October 2010, was assayed for its microbiological composition using fluorescence in situ hybridization (FISH). Briefly, after sample collection, the *I. basta* specimen was cut into tissue strips of approximately 4 cm³, fixed in 4% paraformaldehyde (PFA) for 1 h at room temperature, and stored in ethyl alcohol (EtOH)-phosphate-buffered saline (PBS) (1:1) at -20 °C. For FISH, PFA-fixed samples of *I. basta* were embedded in Neg-50 (Richard-Allan Scientific), a cryogenic water-soluble sectioning medium, and cut to 5-µm thin sections (Leica CM3050 S). We designed specific 16S rRNA-targeted FISH probes for the visualization of '*Ca. Taurinisymbion ianthellae*' (GamD1137, 5'-CTC AAA GTC CCC GCC ATT-3') and the dominant alphaproteobacterial symbiont (AlfD729, 5'-CGGACCTGGCGCCGCTT-3'). To calculate the relative abundance of '*Ca. Taurinisymbion ianthellae*', we applied the double-labeled FISH probe GamD1137 (Cy3), along with the double-labeled FISH probe for the alphaproteobacterial symbiont (AlfD729 in Fluos), and the double-labeled probe mix EUB338-I, EUB338-II, and EUB338-III (all in Cy5; [67]) in equimolar concentrations. *I. basta* sponge section hybridizations were carried out in the presence of 25% formamide in the hybridization buffer (after formamide concentration optimization), and the stringency of the washing buffer was adjusted accordingly [68]. As a negative control, the nonsense probe nonEUB338-I (reverse complementary probe to EUB338-I; double labeled in FLUOS, Cy3, and Cy5) was applied on one section per well per slide hybridized [69]. Probe-conferred visualizations of fluorescent cells were carried out by a confocal laser scanning microscope (CLSM) (LSM 510 Meta; Zeiss, Oberkochen, Germany). Specifically, labeled bacterial cells were counted by eye in 10 randomly selected fields of view (each field contained an average of 260.6 ± 73 SD cells of '*Ca. Taurinisymbion ianthellae*' at 630X magnification with an optical section thickness of 1 µm) on a 146.25 × 146.25 µm ocular grid. Based on these parameters and measurements, we were able to estimate the average density of '*Ca. Taurinisymbion ianthellae*' within the *I. basta* mesohyl, as well as the fraction of '*Ca. Taurinisymbion ianthellae*' relative to total bacterial cells stained by the EUB338 probe mix.

DNA extraction from whole sponge tissue and qPCR for symbiont quantification

Between 80–150 mg of *I. basta* sponge tissue was thawed (if previously frozen at -80 °C), rinsed successively (3x) in 1X calcium- and magnesium-free artificial seawater (CMF-ASW; see Supplementary Note for media details), and immediately ground into a paste with a mortar and pestle in liquid N₂. After resuspension in TE buffer, DNA was extracted from the suspension using the same methods as described elsewhere [10] for DNA extraction prior to symbiont quantification via quantitative PCR (qPCR). DNA was extracted from the two individuals used for metaproteogenomics (see above) as well as three additional yellow thin morphotype healthy individuals from a previous study examining the persistence of microbial symbionts in diseased and healthy specimens of *I. basta* [55]. qPCR was used to quantify the number of 16S rRNA genes of '*Ca. Taurinisymbion ianthellae*', the thaumarchaeal ammonia-oxidizer '*Ca. Nitrosospongia ianthellae*', and the dominant alphaproteobacterial symbiont using specific primers designed for each symbiont phylotype [10].

Phylogenetic analyses

Sequences for the '*Ca. Taurinisymbion ianthellae*' 16S rRNA species tree were assembled by merging a subset of closely related sequences

representing members of sponge specific clusters [70], along with top BLAST hits from representative gammaproteobacterial sequences, and the 16S rRNA sequences from the most closely related members with sequenced genomes. These sequences were aligned via the SINA aligner and the phylogenetic trees constructed in IQ-Tree, version 1.6.2 [71] using the model TN + F + R6 (after model selection using Model Finder; [72] with 10 000 ultrafast bootstraps (UFBoot, [73]). In addition, 16S rRNA gene sequences related to 'Ca. Taurinisymbion ianthellae', were identified in short read archive (SRA) datasets using IMNGS (www.imngs.org, [74]) with default parameters. Successfully mapped reads were then aligned to the reference alignment using SINA and placed into the reference tree using the Evolutionary Placement Algorithm (EPA; [75]) implemented in RAXML-HPC 8.2.11 [76]. Phylogenomic reconstruction was based on a concatenated amino-acid alignment of 43 marker genes constructed with CheckM [64] and trees were constructed using the model LG + F + R7 (after model selection using Model Finder; [72]) with 1000 ultrafast bootstraps (UFBoot, [73]).

Proteomics

Proteome analysis was performed as done previously [10]. In brief, protein extracts were separated by 1D PAGE followed by liquid chromatography-based mass spectrometry (1D-PAGE-LC-MS/MS). MS spectra and MS/MS spectra were acquired from eluting peptides in a LTQ Orbitrap Velos hybrid mass spectrometer (Thermo Fisher Scientific, Waltham, MA, USA) [77, 78], and searched against predicted protein sequence databases composed of the *I. basta* symbiont-enriched metagenome bins and common laboratory contaminants using the Sorcerer SEQUEST (v.27, rev. 11) algorithm. Protein identifications were filtered with Scaffold version 3.5.1 [79]. For protein identification, only peptides identified with high mass accuracy (maximum ± 10 ppm difference between calculated and observed mass) were considered and at least two exclusively unique peptides were required to identify a protein. False-discovery rates (FDRs) were estimated with searches against a target-decoy database [80, 81]. For relative quantitation of proteins, normalized spectral abundance factors (NSAF) were calculated for each sample [82] and averaged for all replicates and samples.

NMR-, LC-MS-based detection and quantification of taurine in *Ianthella basta*

To establish the presence of taurine in *I. basta*, a section of tissue from a yellow thin morphotype was excised by scalpel, weighed wet, and exhaustively extracted with 90% MeOH in MilliQ water. The MeOH extract was lyophilized overnight (DynaVac Freeze-drier). The dry MeOH extract (~5 mg) was dissolved in 1 ml deuterated methanol (CD₃OD; Cambridge Isotope Laboratories) for analysis by proton nuclear magnetic resonance (¹H NMR; Bruker Avance 600 MHz, 5 mm CPTXI inverse ¹H-¹³C/¹⁵N Z-gradient cryogenically cooled probe, referenced to CD₃OD 3.31 ppm, standard 1D zg pulse sequence). Given the crude nature of the extract and the likelihood that the diagnostic signals would be unable to be distinguished from similar chemistry in the extract, 20 mg (dissolved in ~1 ml 50% MeOH) was chromatographed over a pre-equilibrated Strata C18-E 55 μ m, 70 Å, 1000 mg solid phase extraction cartridge (C18-SPE; Phenomenex) and eluted with 10 ml of H₂O, 10% MeOH, 50% MeOH and 100% MeOH. The four fractions (Fractions 1–4) were evaporated under nitrogen stream at 40 °C and lyophilized to dryness. Fractions 1–2 were prepared in 100% deuterated H₂O (D₂O; Cambridge Isotope Laboratories; referenced at 4.39 ppm) and Fractions 3–4 in 10% CD₃OD: 90% CD₃OD (referenced to 3.31 ppm) and analyzed by ¹H NMR. ¹H and COSY NMR spectra of 100 μ M taurine standard, prepared in D₂O, was used to confirm identification of taurine in Fraction 1. Final confirmation was provided by spiking the ¹H NMR sample with 32 μ l and 128 μ l 100 μ M taurine and measuring the increase via integration of the two triplet signals.

To corroborate the NMR assignment, Fraction 1 was also analyzed by LC-MS. A 10 μ l aliquot of the aqueous Fraction 1 was injected onto an Agilent 1100 HPLC system coupled to a Bruker Esquire 3000 Quadrupole Ion Trap LC-MS and eluted from a 150 \times 3 mm Luna 5 μ m NH₂ (Phenomenex) column under the following conditions: 0.8 ml min⁻¹ flow rate; column maintained at 40 °C; mobile phases comprised of H₂O + 0.1% formic acid (A) and MeOH + 0.1% formic acid (B); isocratic elution at 90% A: 10% B for 10 min. The ionspray voltage was set to -4500 V, declustering potential -500V, curtain gas flow 91 min⁻¹, ion source gas 40 PSI, and spray temperature at 350 °C. Data was acquired over the mass range 70–200 *m/z*; product ion MS/MS data was acquired over 50–200 *m/z* to establish the fragmentation pattern. Retention time as well as total and extracted ion chromatographs (positive mode) were compared against a 100 μ M taurine standard prepared in MilliQ.

The concentration of taurine in sponge tissue was measured by quantitative NMR (qNMR) [83]. Briefly, five sponge explant samples were extracted and chromatographed over C18-SPE as described above. ¹H NMR spectra of Fraction 1 (~16 mg dry extract) from each of the five sponge extracts were acquired in 800 μ l D₂O (δ H 4.39) at 298 K, with sweep width 12 ppm (7184 Hz), 90° pulse, 35 s relaxation delay, receiver gain 16, 2 dummy scans, 16 acquisition scans and 64 k data points. The external reference signal was calibrated using a stock solution of 2 mM taurine in D₂O. The concentration of taurine in the NMR samples was determined by comparing the signal integrals of well resolved non-exchangeable protons (2H) centered at 3.26 ppm in a 0.20 ppm window, with that of the reference signal. Concentration was normalized to sponge wet wt.

Taurine measurement in sponge tissue "pore water"

Taurine concentration was measured in readily extractable water, referred to as pore water, from sponge tissue samples of three yellow thin *Ianthella basta* individuals from Davies Reef. The pore water samples of freshly collected *I. basta* tissue samples (approx. 1 \times 0.5 cm; 0.54 \pm 0.08 g sponge wet wt) were obtained using the following two methods: first, tissue samples were placed in 2.5 ml plastic syringe barrels (after removal of the plunger) and pore water was squeezed into 2 ml plastic collection tubes by applying pressure with the syringe plunger. For the second method, fresh tissue samples were placed into 0.5 ml plastic centrifuge tubes with perforated bottoms (5 holes punched with a 23 G needle). The perforated tubes were placed into 2 ml plastic collection tubes, and *I. basta* pore water was collected via centrifugation at 1000 g for 1 min. All collected pore water samples were immediately frozen and stored at -80 °C until further analysis.

For taurine analysis, the pore water samples (*n* = 6) were diluted 1:10 in artificial seawater (per l: 26.4 g NaCl, 6.8 g MgSO₄*7H₂O, 5.7 g MgCl₂*6H₂O, 1.47 g CaCl₂*2H₂O, 0.66 g KCl, 0.2 g KH₂PO₄, 0.19 g NaHCO₃), and the remaining debris in diluted pore water samples was pelleted by centrifugation at 10,000 g for 5 min. Taurine in the clear supernatant of the *I. basta* pore water samples was quantified against a taurine standard (0 to 250 μ M) prepared in artificial seawater. Samples and standards were derivatized with the AccQ-Tag Ultra Derivatization Kit (Waters™) and subsequently measured on a UPLC-Orbitrap mass spectroscopy system [84] with modifications to the UPLC settings. In brief, samples were measured using a UPLC Ultimate 3000 system (Thermo Fisher Scientific, Bremen, Germany) linked to an Orbitrap Q Exactive HRMS system (Thermo Fisher Scientific) with an electrospray ionization (H-ESI) source. Chromatographic separation was conducted on a Water AccQ-Tag Ultra C18 column (2.1 \times 100 mm, 1.7 μ m particles; Milford, MA, USA) with an ACQUITY column in-line guard filter (2.1 mm, 0.2 μ m; Milford, MA, USA) at 55 °C column temperature. The mobile phase consisted of 0.001% formic acid in MilliQ (eluent A) and 0.001% formic acid in acetonitrile (eluent B). The following solvent gradient was applied: 0–0.5 min kept constant at 0.1% B, 0.5–2.5 min increased to 5% B, 2.5–8 min increased to 20% B, 8–8.25 min increased to 90% B, 8.25–11 min maintained at 90% B, 11–11.2 min decreased to 0.1% B, and 11.2–4.5 min maintained at 0.1% B for column re-equilibration. The flow rate was set to 0.4 ml min⁻¹ and the injection volume was 1 μ l. The Orbitrap Q Exactive HRMS system was operated using full-mass scan mode (*m/z* 150–1000) in the ESI positive mode. The automatic gain control (AGC) target values were set to 3 \times 10⁵ and the resolution was set to 70,000. The lock mass correction was set to 214.0896 (contaminant from plasticizer). The spray voltage was 3.5 kV, while the capillary temperature was set to 300 °C. The sheath gas consisted of 35 arbitrary units, and the auxiliary gas of 15 arbitrary units.

Isotopic analysis of whole sponge tissue, total nucleic acids, and ¹⁵N in NH₄⁺ & NO₂⁻ using EA-IRMS

For the determination of ¹³C- and ¹⁵N-enrichment within the holobiont, sponge tissue samples were rinsed briefly (3x) in 1X CMF-ASW, freeze-dried, ground to a fine powder in a mortar, and stored dry, prior to analysis. $\delta^{13}\text{C}$ - and $\delta^{15}\text{N}$ -values of sponge tissues were determined by an elemental analyzer (EA 1110, CE Instruments, Milan, Italy) coupled to an isotope ratio mass spectrometer (IRMS; Finnigan MAT Delta^{plus} IRMS with a Finnigan MAT ConFlo III interface). For determination of ¹³C- and ¹⁵N-enrichment in total nucleic acids, *I. basta* whole sponge tissue was homogenized using the above procedure employing liquid N₂, followed by nucleic acid extraction according to the procedures outlined in [85]. The extracted nucleic acids were then dried overnight in an oven, and $\delta^{13}\text{C}$ - and $\delta^{15}\text{N}$ -values were determined via the same procedure as above. For quantification of the amount of ¹³C- and ¹⁵N-derived taurine that was incorporated into *I. basta*

holobiont biomass, the following formulas were used:

$$n_{C,taurine} = \frac{(a_{13C,sponge} - a_{13C,ctrl})}{(a_{13C,taurine} - a_{13C,ctrl})} n_{C,total}$$

$$n_{N,taurine} = \frac{(a_{15N,sponge} - a_{15N,ctrl})}{(a_{15N,taurine} - a_{15N,ctrl})} n_{N,total}$$

where the displayed symbols, abbreviations and designations refer to: a — isotope fraction $^{13}C/(^{12}C + ^{13}C)$ or $^{15}N/(^{14}N + ^{15}N)$ given in at%; n : number of carbon or nitrogen elemental atoms; *sponge* — sponge material; *ctrl* — natural isotope abundance control; *total* — total amount of carbon or nitrogen in the analyzed sample. The denominator in both equations ($a_{15C,N,taurine} - a_{15C,N,ctrl}$) were calculated via a standard two-pool mixing model [86]. For comparability of the measurement values obtained from distinct incubations, n was normalized to the wet weight of the utilized *I. basta* explants.

For ^{15}N -analysis of NH_4^+ and NO_2^- , sampled seawater from the glass tanks with the labeled taurine incubations was filtered through pre-combusted GF/Fs (Whatman International; treated for 4 h at 450°C), and subsequently through 0.2 µm polycarbonate filters (Sartorius). All samples were immediately frozen at -20°C for later analysis. Prior to shipment to the University of Vienna, samples were thawed at room temperature and the microbial inhibitor phenylmercuric acetate was added (to a final concentration of 10 µM). Upon arrival in Vienna, the samples were promptly stored at -80°C. For determination of the ^{15}N content in ammonia, NH_4^+ was extracted from samples via microdiffusion [10, 87]. Briefly, 100 mg MgO and an acid trap (acidified cellulose filter disc enclosed in a semi-permeable Teflon membrane) were added to 9 ml of sample and 1.5 ml of 3 M KCl. After 5 days shaking at 35°C, the acid traps were removed, dried over concentrated sulfuric acid, and analyzed for the ^{15}N content by an elemental analyzer (EA 1110, CE Instruments, Milan, Italy) coupled to an isotope ratio mass spectrometer (IRMS; Finnigan MAT Delta Plus IRMS with a Finnigan MAT ConFlo III interface). The nitrogen isotope composition of NO_2^- was determined by a method based on the reduction of NO_2^- to N_2O by using sodium azide under acidified conditions [88]. Briefly, 1 ml sample or standard was transferred to 12 ml exetainer and 1 ml 1 M HCl was added. After purging the vials with helium to expel air- N_2O from the sample headspace, 150 µl 1 M sodium azide buffer (in 10% acetic acid solution) was injected and the vials were placed on a shaker at 37°C for 18 h. The reaction was quenched by injecting 250 µl of 10 M NaOH. Derived N_2O was analyzed using a purge-and-trap GC/IRMS system (PreCon, GasBench II headspace analyzer, Delta Advantage V IRMS; Thermo Fischer). Similar to the above calculations, the amount of taurine-derived NH_4^+ and NO_2^- were calculated as follows:

$$n_{NH_4^+,taurine} = \frac{(a_{15N,NH_4^+} - a_{15N,ctrl})}{(a_{15N,taurine} - a_{15N,ctrl})} n_{NH_4^+,total}$$

$$n_{NO_2^-,taurine} = \frac{(a_{15N,NO_2^-} - a_{15N,ctrl})}{(a_{15N,taurine} - a_{15N,ctrl})} n_{NO_2^-,total}$$

By taking into account that the isotopically labeled nitrite emerges from oxidation of ammonia obtained from taurine dissimilation, the total amount of NH_4^+ released by the holobiont through taurine metabolism was calculated via:

$$n_{NH_4^+,released} = \left(n_{NH_4^+,taurine,sponge} - n_{NH_4^+,taurine,SW} \right) + \left(n_{NO_2^-,taurine,sponge} - n_{NO_2^-,taurine,SW} \right)$$

where SW refers to the values determined from control incubations utilizing seawater without sponge explants. For comparability of the measurement values obtained from distinct incubations, n was normalized to the wet wt of the utilized *I. basta* explants.

NanoSIMS analysis of *Ianthella basta*

NanoSIMS measurements were undertaken on two of the three *I. basta* explant samples obtained from the $^{13}C^{15}N$ -taurine incubations. Specimens were selected for maximum isotope enrichment, based on results from EA-IRMS bulk analysis (0.62 and 0.55 at% ^{15}N ; 1.19 and 1.15 at% ^{13}C). Briefly,

approximately 0.5 cm³ sections were cut from *I. basta* samples, which had been fixed in 4% PFA and stored in a 1:1 mixture of PBS and 96% ethanol at -20°C. The thus obtained specimens were then rinsed successively (3x) in 1X calcium- and magnesium-free artificial seawater (CMF-ASW) and gently dissociated in 1X CMF-ASW with a scalpel, mortar and pestle, and a final step of sonication for two 30 s cycles at 35% power using a sonication probe [Sonopuls HD2200 equipped with probe MS73 (output frequency 20 kHz, power 200 W, amplitude: 310 µm), Bandelin, Germany]. The suspensions were then filtered through 0.45 µm cellulose acetate filters (type Minisart, Sartorius, Göttingen, Germany) to remove a large portion of remaining sponge cells and nuclei (microscopic visualizations showed a lack of sponge nuclei after filtration), centrifuged at 10,844 × g for 10 min at 4°C to pellet cells, and resuspended in 50% EtOH/50% 1X PBS solution. To visualize all DNA-containing cells present in the sample, a 30 µl aliquot of the suspension was spotted onto antimony-doped silicon wafer platelets (7.1 × 7.1 × 0.75 mm; Active Business Company, Germany) and dried at 46°C, before staining with a 0.1 % (w/v) solution of the DNA-binding dye 4,6-diamidino-2-phenylindole (DAPI) (Sigma, Deisenhofen, Germany) at room temperature for 5 min. Excess DAPI was removed by rinsing with distilled water and the slides were air-dried. Samples were then imaged on an epi-fluorescence laser microdissection microscope (LMD, Leica LMD 7000) using a 40x air objective for pre-selection of suitable NanoSIMS measurement areas, which were subsequently marked utilizing the LMD laser. High resolution imaging of fluorescent cells in marked regions was carried out in a confocal laser scanning microscope (CLSM) (LSM 510 Meta; Zeiss, Oberkochen, Germany). NanoSIMS measurements were performed on a NanoSIMS 50 L (Cameca, Gennevilliers, France) at the Large-Instrument Facility for Environmental and Isotope Mass Spectrometry at the University of Vienna. Further details on NanoSIMS data acquisition and analyses are presented in the Supplementary Information.

RESULTS AND DISCUSSION

A metagenome assembled genome and phylogenetic analyses of the dominant gammaproteobacterial symbiont of *Ianthella basta*

From the extensive metagenomic data set used for genomically characterizing the thaumarchaeal symbiont of *I. basta* [10], we retrieved a 2.35 Mbp MAG consisting of 97 contigs, representing a nearly complete genome (94.8%; possibly originating from several closely related strains) with a very low level of contamination (Table S1). Phylogenetic analysis of the only 16S rRNA gene copy in the MAG demonstrated that this gene specifically clustered at 99% nucleotide identity with previously recovered sequences of the dominant gammaproteobacterial symbionts from *I. basta* (Fig. S1) [10, 55, 56] and fall into the neighborhood of sponge specific clusters 144–8 (SC) [70]. A phylogenomic reconstruction using concatenated single copy conserved marker genes (Fig. 1) [64], confirmed the affiliation of this MAG with the Gammaproteobacteria and revealed that it can be further classified into the Arenicellales order and within the LS-SOB family (originally named after the bacterial MAG extracted from the glass sponge *Lophophysema eversa*, which encodes a sulfur oxidation pathway [89]; based on the Genome Taxonomy Database [90]).

Based on the concatenated gene tree analyses, we further queried representative 16S rRNA gene sequences pulled from LS-SOB genome bins, against the IMGs 16S rRNA gene amplicon database [74], and placed the hits into the reference 16S rRNA gene tree using the Evolutionary Placement Algorithm [75]. As a result, 3 sets of short reads were placed into the branch leading to the dominant gammaproteobacterial symbiont sequences obtained from *I. basta* (Fig. S1). The closest two groups (I4, I6) comprised 5 (out of 6 total) operational taxonomic unit (OTU) reads derived from unspecified coral and sponge samples, 4 of which were OTU reads from corals sampled from the same study site as *I. basta* for this study (Orpheus Island, Queensland, Australia). 141 OTU reads were placed into the I7 group, of which 29 and 4 were derived from sponge and coral metagenomes, respectively (the other 112 OTU reads were derived from other metagenomic data sets spanning a variety of environmental

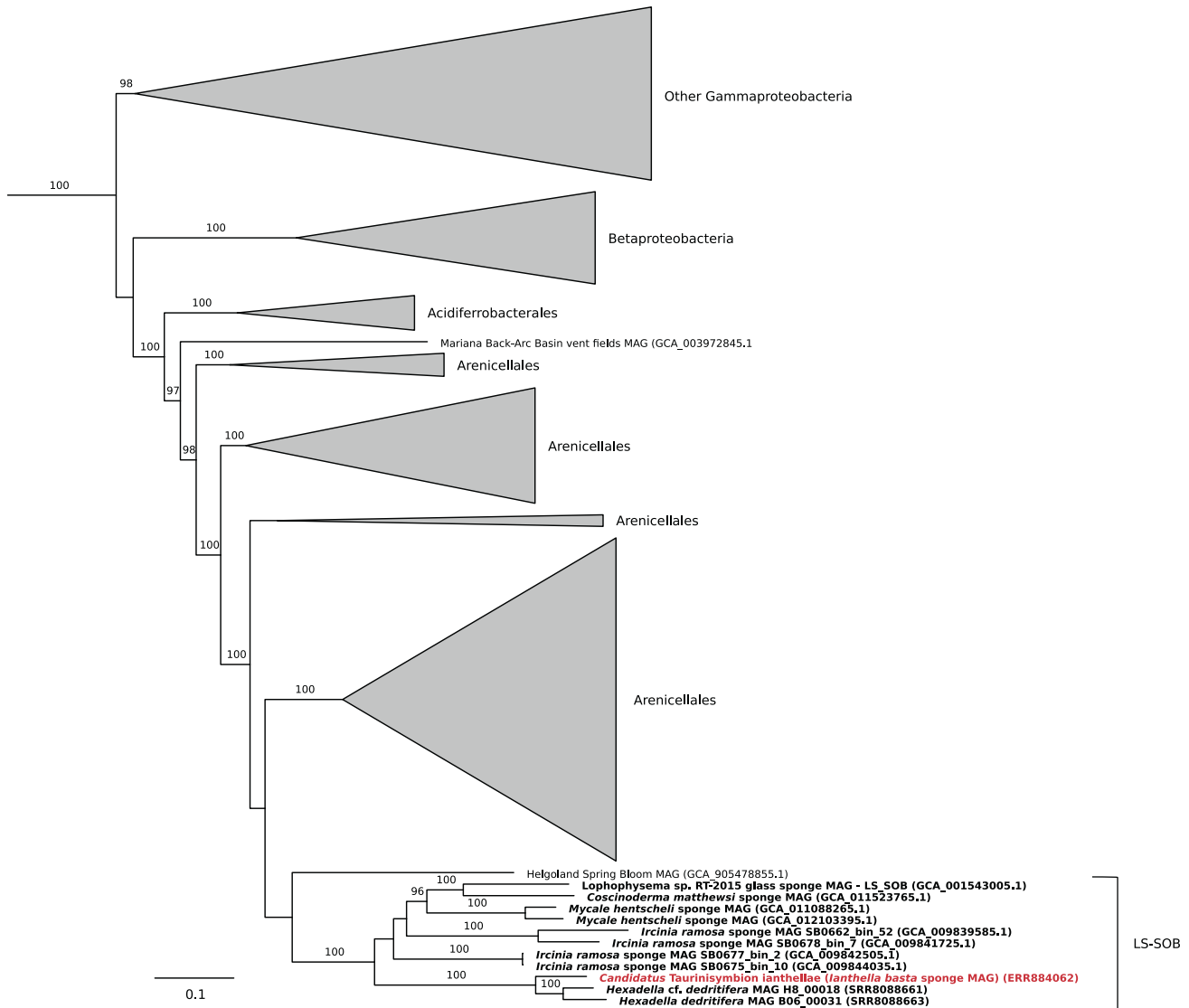


Fig. 1 Maximum-likelihood phylogenomic tree of ‘*Ca. Taurinisympion ianthellae*’ along with other selected proteobacterial symbionts. The phylogenomic tree is based on 43 concatenated universal, single-copy marker genes identified with CheckM, and was generated after automatic model selection with IQ-Tree. ‘*Ca. Taurinisympion ianthellae*’ is displayed in red bold font while sponge symbionts are displayed in black bold font.

matrices). Out of this group, three OTU reads were obtained from two sympatric marine sponge species (NE Atlantic) within the same genus, (*Hexadella deditifera* and *Hexadella cf. deditifera*), both of which are also affiliated with the same sponge family as *I. basta*, the Ianthellidae. These two closely related phylotypes, from *H. deditifera* and *H. cf. deditifera*, respectively, exhibited 16S rRNA gene identities of ~97% (over 418 bp) with each other, 95–97% with the *I. basta* gammaproteobacterial symbiont, and were found to comprise 33–42% of the total amplicon dataset derived from these sponges [91]. Noting that these two *Hexadella* species harbor abundant and closely related gammaproteobacterial phylotypes, and also contain AOA-symbionts closely related to the AOA in *I. basta* [66], we assembled and binned two new gammaproteobacterial symbiont MAGs from the published raw read data set of these two *Hexadella* sponges.

The phylogenomic reconstruction confirmed that these two *Hexadella* gammaproteobacterial symbiont MAGs were most closely related to the *I. basta* gammaproteobacterial symbiont (Fig. 1), and AAI analyses indicated that the *I. basta* gammaproteobacterial symbiont shares AAI values of 76–80% with these two

Hexadella gammaproteobacterial symbionts. Among the other LS-SOB genomes retrieved from marine sponges [37, 89, 92–94], the *I. basta* gammaproteobacterial symbiont shares AAI values of 54–59%. Since these identity values signify that the gammaproteobacterial symbiont represents a new species within a new genus along with the other two *Hexadella* gammaproteobacterial symbionts — 60–80% AAI is typical for organisms grouped at the genus level [95, 96] — we propose the name ‘*Candidatus Taurinisympion ianthellae*’. *Taurinisympion* gen. nov. (Tau.ri.ni.sym’bi.on. N.L. n. taurinum, taurin; Gr. pref. sym, together; Gr. masc. part. n. bion, a living being; N.L. masc. n. *Taurinisympion*, a taurin-degrading living partner) for the *I. basta* gammaproteobacterial symbiont. The name *Taurinisympion* describes this organism’s ability to utilize taurine as a source of energy and biomass whilst residing in symbiosis within a sponge, and we were able to identify the same pathways encoded by ‘*Ca. Taurinisympion ianthellae*’ for taurine utilization in the two *Hexadella* gammaproteobacterial symbiont MAGs, thereby suggesting a conserved evolutionary function that may be adaptive for this proposed genus (see below; Table S2). The species name

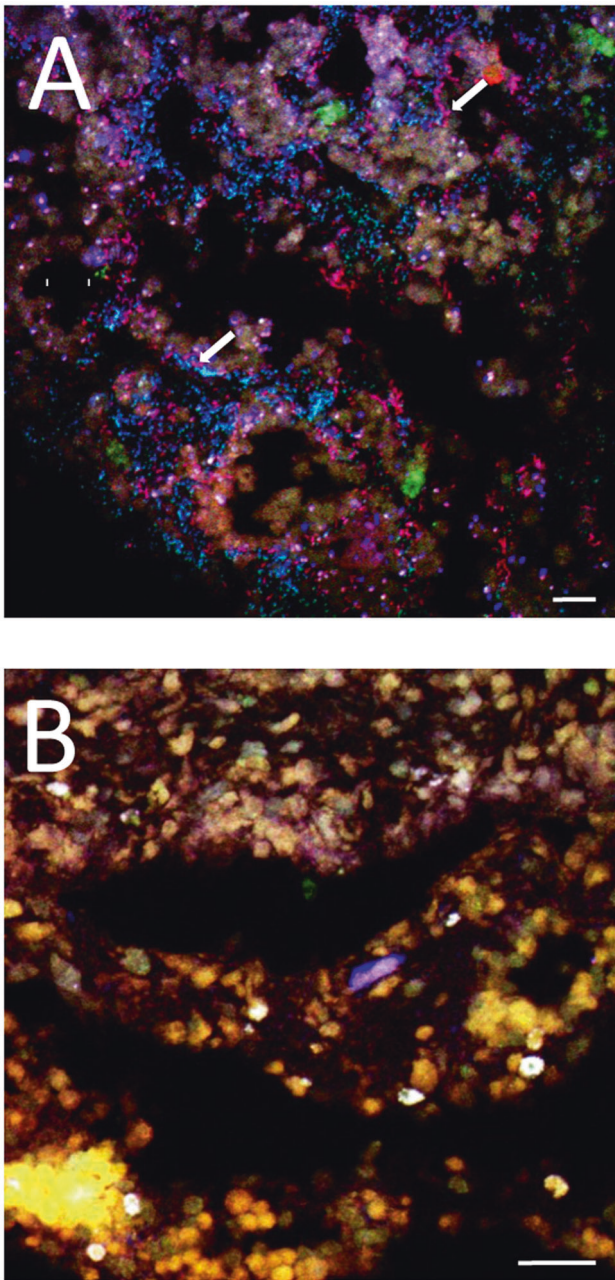


Fig. 2 Fluorescence in situ hybridization of 5 µm thick cryosections of *Ianthella basta* using double-labeled probe sets. **A** '*Ca. Taurinisymbion ianthellae*' (red), *Alphaproteobacteria* symbiont-probe (green), and *Bacteria*-probe (EUB338-I-III; blue); **B** negative controls using the double-labeled non-EUB338 probe set are depicted in all three color channels. The combination of the '*Ca. Taurinisymbion ianthellae*' specific probe signals in red with the general *Bacteria* probe signals in blue, results in the visualization of '*Ca. Taurinisymbion ianthellae*' as magenta signals and representative cells are indicated with white arrows. The alphaproteobacterial symbiont appears in cyan. Green structures represent autofluorescence. Scale bars are 10 µm for reference.

ianthellae refers to its discovery and description as a symbiont of the marine sponge, *I. basta*.

'*Candidatus Taurinisymbion ianthellae*' is an abundant symbiont of *Ianthella basta*

Consistent with the high coverage of reads and peptides assigned to '*Ca. Taurinisymbion ianthellae*' in the metaproteogenomic data

sets from *I. basta* and the dominance of this phylotype in other *I. basta* studies [54–56], we observed a high abundance of this symbiont (Fig. 2) in the mesohyl of *I. basta* using fluorescence in situ hybridization (FISH) with a newly designed specific 16S rRNA-targeted probe. Quantitative FISH revealed that '*Ca. Taurinisymbion ianthellae*' achieved average cell densities of 1.22 ± 0.34 (SD) $\times 10^{10}$ cells cm^{-3} sponge and accounted for $24 \pm 5.6\%$ (SD) of all cells hybridizing with the probe set EUB338-I-III targeting most bacteria (which does not cover the thaumarchaeal symbiont of *I. basta*). Moreover, absolute quantification of '*Ca. Taurinisymbion ianthellae*' using qPCR with newly designed symbiont specific primers, showed an average absolute abundance of 2.78 ± 1.5 (SD) $\times 10^{10}$ 16S rRNA gene copies g^{-1} sponge wet wt, which is in the same range as the population density values observed from the FISH images (assuming that 1.2 g sponge wet wt = 1 cm^{-3} ; [97]). The absolute abundances obtained for the dominant thaumarchaeal and alphaproteobacterial symbionts are also in the 10^{10} 16S rRNA gene copies g^{-1} sponge wet wt range (Fig. S2). The ratio of '*Ca. Taurinisymbion ianthellae*' 16S rRNA sequences to the total 16S rRNA genes derived from qPCR assays (targeting the gammaproteobacterial-, alphaproteobacterial-, and thaumarchaeal symbionts of *I. basta*) was 41.1 ± 34 (SD)%. Nevertheless, it should be noted that qPCR abundances cannot directly be translated to cell numbers as (i) symbionts can have multiple rRNA gene copies (although the '*Ca. Taurinisymbion ianthellae*' MAG has only one 16S rRNA gene copy), (ii) genome polyploidy might occur in sponge symbionts and (iii) extracellular DNA of the symbionts will also be detected. Similarly, using FISH for quantification may result in the undercounting of microbial cells with low ribosome contents.

'*Ca. Taurinisymbion ianthellae*' expresses proteins for taurine catabolism and subsequent NH_4^+ and SO_4^{2-} export

To analyze the metabolic potential of '*Ca. Taurinisymbion ianthellae*', we annotated its MAG by employing the previously presented metaproteogenomic data set from *I. basta* [10] and were able to assign 149 proteins to this symbiont MAG. These proteins represented 35.7%, in NSAF values, of all proteins assigned to the *I. basta* microbiome (Table S3), highlighting the physiological dominance of '*Ca. Taurinisymbion ianthellae*'. From this metaproteogenomic dataset, we concluded that '*Ca. Taurinisymbion ianthellae*' is a facultative anaerobe with an ability to metabolize a variety of organic compounds. The genomic potential for the major central metabolic pathways, such as glycolysis, the pentose phosphate pathway, the tricarboxylic acid (TCA) cycle, the glyoxylate bypass, a conventional respiratory chain (complex I–IV; two respiratory complex IV were found to be encoded, a *cbb₃*- and a *aa₃*-type cytochrome c oxidase; complex V), and the genes for denitrification of NO_2^- to N_2O , and DMSP catabolism, were all present in the recovered MAG (Fig. 3, Table S2). A further discussion of a few of these genomic features, with a focus on DMSP metabolism, is provided in the Supplementary Information.

'*Ca. Taurinisymbion ianthellae*' encodes a previously described pathway for taurine import and transamination (*tauABC*, *tpa*, *xsc*) [98] into sulfite via a desulfonated intermediate sulfoacetaldehyde, as well as a pathway for the subsequent oxidation of the resultant toxic and highly reactive sulfite into sulfate via the cytoplasmic enzymes APS reductase (*aprAB*) and ATP sulfurylase (*sat*) [58]. This pathway consumes AMP and sulfite, and releases ATP via substrate-level phosphorylation and sulfate, while channeling two electrons from the oxidation of sulfite, with its very negative redox potential, to the quinone pool via the membrane-bound QmoAB. Consistent with other sulfur oxidizing bacterial genomes, the *qmoC* gene is replaced by *hdrBC* genes ([99] and references therein), with the *hdrBC* genes found to be adjacent to *qmoAB* in '*Ca. Taurinisymbion ianthellae*', and the HdrB subunit expressed in the holobiont (Fig. 3, Tables S2 and S3). For

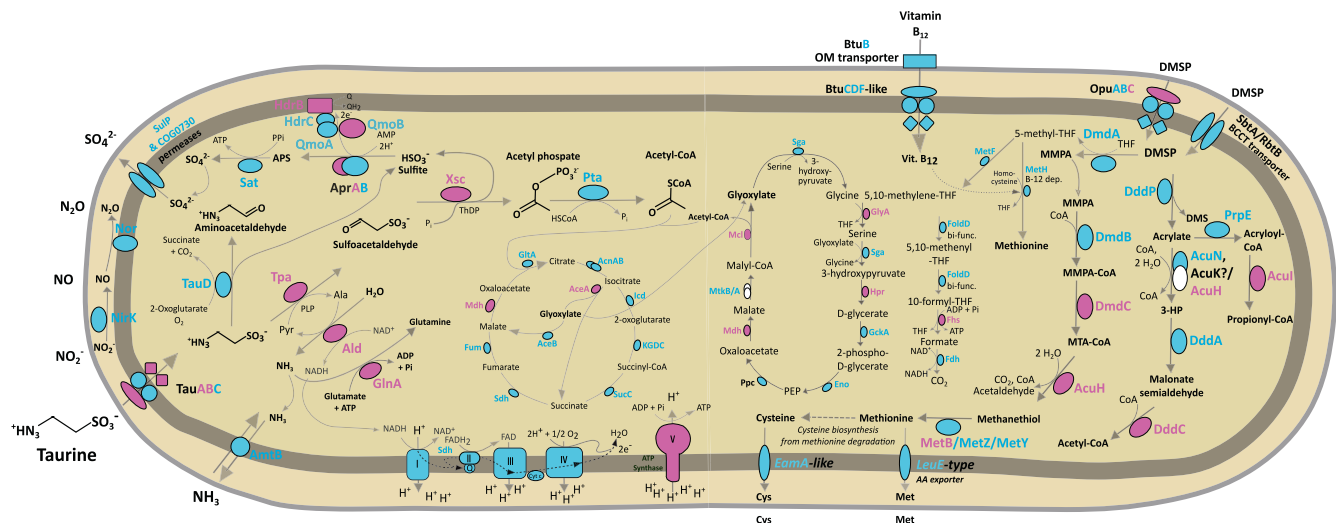


Fig. 3 Taurine and DMSP metabolic pathways identified and expressed in ‘*Ca. Taurinisymbion ianthellae*’. Central carbon and nitrogen metabolism in ‘*Ca. Taurinisymbion ianthellae*’ based on metaproteogenomic analyses with a focus on taurine and DMSP metabolism pathways along with the relevant import and export of exchanged metabolites. Depicted are proteins necessary for taurine import, followed by taurine dissimilation, energy conservation via sulfite oxidation and the electron transport chain, along with carbon incorporation via the glyoxylate bypass. Similarly depicted are the proteins necessary for DMSP import as well as the corresponding DMSP cleavage and demethylation pathways, including the oxidation of 5-methyl-THF and its role as a carbon donor for the conversion of glycine to serine. Enzymes detected via metaproteomics are highlighted in fuchsia, while enzymes only identified in the ‘*Ca. Taurinisymbion ianthellae*’ MAG are highlighted in turquoise. Missing pathway genes are depicted as white shapes. AMP adenosine monophosphate, APS adenosine-5'-phosphosulfate, Cys cysteine, DMSP dimethylsulfoniopropionate, DMS dimethylsulfide, 3-HP 3-hydroxypropanoate, Met methionine, MMPA methylmercaptopyruvate, MTA-CoA methylthioacryloyl-Coenzyme A, PEP phosphoenolpyruvate, PLP pyridoxal 5'-phosphate, Q quinone, ThDP thiamine diphosphate, THF tetrahydrofolate. Additional information for genes and pathways depicted in the figure can be found in Supplementary Tables S2–S5.

the potential export of sulfate, two putative sulfate permeases (COG0730 permease family, [100]; COG0659, SulP family permease), were detected in the ‘*Ca. Taurinisymbion ianthellae*’ MAG. The gene encoding taurine dioxygenase (*tauD*), an alpha-ketoglutarate-dependent dioxygenase, which desulfonates taurine into aminoacetaldehyde (the fate of which is currently unknown) and sulfite, was also found within the ‘*Ca. Taurinisymbion ianthellae*’ MAG. TauD is involved in the assimilation of sulfur from taurine in several aerobic bacteria [101]. Furthermore, we found many of these genes (*tauABC*, *tpa*, *tauD*, *xsc*, *aprAB*, *qmoABC*) encoded in the previously mentioned Hexadella gammaproteobacterial symbiont MAGs, which belong to the same proposed genus as ‘*Ca. Taurinisymbion ianthellae*’ (Table S2).

Several of the genes involved in taurine degradation were also found to be expressed after being mapped to the ‘*Ca. Taurinisymbion ianthellae*’ MAG. Specifically, we detected the expression of the taurine transporter TauABC (with TauAB detected only when the 454 metagenome dataset was included as a database for initial metaproteomic analyses), and the two enzymes, taurine-pyruvate aminotransferase (*Tpa*) and sulfoacetaldehyde acetyltransferase (*Xsc*), involved in the sequential dissimilation of taurine to sulfite via sulfoacetaldehyde. Additionally, 3 out of 7 proteins necessary for the subsequent oxidation of sulfite to sulfate (*AprA*, *QmoB* and *HdrB*); while *Sat* was not detected in the metaproteome data set) were expressed. A phosphate acetyltransferase is present in the ‘*Ca. Taurinisymbion ianthellae*’ MAG, which would convert the acetyl phosphate produced from the activity of *Xsc* (also producing sulfite) into acetyl-CoA, for entry into the TCA and the glyoxylate bypass cycle. We detected the expression of the key enzymes malate dehydrogenase (*Mdh*) and isocitrate lyase (*AceA*), from each cycle, respectively, suggesting that the glyoxylate bypass is used for anabolic purposes, while sulfite oxidation is used for energy conservation by ‘*Ca. Taurinisymbion ianthellae*’. In addition to the expressed proteins detected for the processing of taurine-derived sulfur and carbon compounds, we detected the expression of

alanine dehydrogenase (*Ald*), which would replenish the pyruvate needed by the *Tpa* enzyme for taurine dissimilation (while also providing NADH/H⁺ for respiration) and provide NH₃ for assimilation into glutamine, by a highly expressed glutamine synthetase (*GlnA*; 1.30% NSAF). Ammonia can also be transported out of the cell via an encoded ammonium transporter (*amtB*; Fig. 3, Table S2), where it can be readily oxidized to nitrite, as previously demonstrated [10], by the dominant thaumarchaeal symbiont. Excluding the expression of glutamine synthetase, the other detected 6 proteins involved in the catabolism of taurine (*Tpa*, *Xsc*, *AprA*, *QmoB*, and *HdrB*) amounted to 0.97% NSAF of the 149 proteins assigned to the ‘*Ca. Taurinisymbion ianthellae*’ MAG. Nevertheless, the detection of the high affinity *GlnA* suggests that ‘*Ca. Taurinisymbion ianthellae*’ was nitrogen limited at the time that the *I. basta* holobiont individual was sampled in situ. It has been previously observed that the *I. basta* holobiont, along with its thaumarchaeal ammonia-oxidizing symbiont, ‘*Ca. Nitrosospongia ianthellae*’, is nitrogen limited at ambient conditions [10], and this is in line with apparent nitrogen limitation in marine systems [102] and mammalian large intestines [103]. The observations that the *I. basta* holobiont readily dissimilated added taurine in *I. basta* explant incubations (see below) and incorporated the taurine-derived carbon and nitrogen at C:N ratios indicative of nitrogen limitation (see Supplementary Information), further corroborate these findings.

While the expression of the taurine transporter has been observed in the gammaproteobacterial symbiont of *Olavius algarvensis* [104], the recent observations that marine sponge symbionts have the capacity for taurine utilization, is primarily based on gene presence [25, 26, 35–37], with the exception of metaproteomic evidence for *Ca. Entotheonella* phylotypes residing in the marine sponge *Theonella swinhoei*. However, this symbiont expressed multiple encoded copies of TauD-related proteins postulated to possibly function in the breakdown of small aromatic compounds [105]. A recent study by our group performed deep sequencing runs on more *I. basta* individuals — while also

conducting metaproteomics — and was able to assemble additional low abundant microbial symbiont MAGs that were previously overlooked [106]. One of these low abundant symbionts is an alphaproteobacterium (Alphaproteobacteria, g_UBA2767) that also possesses the capability to fully convert taurine into ammonium and sulfate via the same pathways as ‘*Ca. Taurinisymbion ianthellae*’. However, this low abundance Alphaproteobacterium only represents 1–5% of the microbial community and did not express any of the proteins involved in taurine import, taurine dissimilation or sulfite oxidation (it only expressed 0.4% of all detected proteins in the metaproteomic dataset). Moreover, this set of metaproteomic analyses was able to detect the TauABC and AprA proteins and definitively assign them to the ‘*Ca. Taurinisymbion ianthellae*’ MAG.

Oxidation of sulfite to sulfate by taurine-degrading bacteria occurs via different pathways. Frequently periplasmic and cytoplasmic sulfite dehydrogenases are used [107, 108], but these enzymes were not detected in the ‘*Ca. Taurinisymbion ianthellae*’ MAG. The genetic capability to carry out the two-step AMP-dependent indirect oxidation of sulfite to sulfate via APS in the cytoplasm employed by this symbiont, is infrequently detected in taurine degraders, with examples found among the ubiquitous, pelagic SAR11 ([58]; but most SAR11 lack ATP sulfurylase), the γ -3 symbiont in the gutless oligochaete, *Olavius algarvensis* [109], and two marine sponge symbionts [25, 26]. Although a metaproteomic study in Antarctic waters has previously revealed the expression of SAR11-associated peptides for this particular pathway of taurine dissimilation (Tpa, Xsc) followed by sulfite oxidation (AprAB) [58], SAR11 in culture has not yet been shown to excrete sulfate in the presence of taurine [110, 111].

Taurine metabolism in the *Ianthella basta* holobiont

Based on the findings of the metaproteogenomic data set, we investigated taurine metabolism in the *I. basta* holobiont experimentally. NMR and LC-MS analyses of the 90% MeOH extract and the aqueous Fraction 1 confirmed that taurine was present in this sponge (Fig. 4A and Fig. S3) [112]. The natural concentration of taurine, determined by qNMR, was $5.48 \pm 0.69 \mu\text{mol g}^{-1}$ sponge wet wt, which is in the mid-range of previously reported values for six other marine sponges (1.05 – $12.5 \mu\text{mol g}^{-1}$ sponge wet wt sponge) [113]. Furthermore, taurine measurements in *I. basta* pore water samples ranged between $819 \mu\text{M}$ and $1352 \mu\text{M}$, with no significant difference (t-test, $p = 0.2754$) between the two pore water extraction methods employed. Congruently, we were able to detect ^{13}C and ^{15}N enrichment in whole sponge and total nucleic acids elemental analyzer isotope ratio mass spectrometry (EA-IRMS) analyses of *I. basta* sponge explants that underwent additions of an equimolar mixture of ^{13}C - and ^{15}N -labeled taurine in 48 h incubations (Fig. 4B and Fig. S4). While it cannot be excluded that sorption of labeled taurine contributed to the isotopic enrichment in the whole sponge experiments, the detection of labeled total nucleic acids clearly indicated assimilation and incorporation of labeled taurine into *I. basta* holobiont biomass. Thus, from the whole sponge EA-IRMS data, we were able to estimate uptake rates of taurine-derived C and N assimilated into whole *I. basta* holobiont biomass and obtained values of $1.38 \pm 0.3 \text{ nmol C min}^{-1} \text{ g}^{-1}$ sponge wet wt (\pm SE) and $0.74 \pm 0.2 \text{ nmol N min}^{-1} \text{ g}^{-1}$ sponge wet wt (\pm SE). These *I. basta* holobiont taurine-derived carbon uptake rates correspond to approximately 4–10% of the bulk DOC uptake rates reported for the more diverse microbiome of the marine sponge *Aplysina aerophoba* [17], thereby highlighting the importance of taurine in the *I. basta* holobiont. Moreover, NanoSIMS analyses conducted on dissociated sponge extracellular material revealed accumulation of taurine-derived C and N within regions (Figs. S5 and S6) that were similar in size and shape to typical sponge microbial symbiont cells previously visualized in *I. basta* by transmission electron microscopy [55, 114].

Taurine catabolism by *Ianthella basta* holobiont results in the accumulation of inorganic S and N species

Some microbial pure cultures catabolizing taurine, oxidize the dissimilated sulfonate moiety to sulfate, which is subsequently excreted [115–117]. Considering that metaproteogenomic analyses predicted sulfate as a secreted end product of ‘*Ca. Taurinisymbion ianthellae*’ taurine metabolism, we analyzed whether the *I. basta* holobiont produced sulfate (SO_4^{2-}) in experiments with and without added taurine. Specifically, we conducted 48 h incubations with *I. basta* explants amended with taurine (in total 1.6 mM) and without taurine in SFASW. SFASW was used in these incubations to facilitate the detection of sulfate formation by the holobiont. Pairwise comparisons in incubations with sponges in SFASW without the addition of taurine (SFASW + *I. basta*), resulted in a small, but significant production of SO_4^{2-} after 12 h, indicating in vivo production of SO_4^{2-} ($p < 0.05$, one-tailed t-test) (Fig. 5A). In incubations with *I. basta* explants and added taurine (SFASW + *I. basta* + taurine), we observed a similarly small increase at 12 h ($p < 0.05$, one-tailed t-test), with SO_4^{2-} production strongly increasing between the 12 h and 48 h time points, suggesting a metabolic lag effect (Fig. 5B). Moreover, the final SO_4^{2-} concentrations of 590 ± 89 (SE) μM SO_4^{2-} ($59.0 \pm 2.0 \mu\text{mol g}^{-1}$ sponge wet wt in Fig. 5A) at 48 h were significantly higher than the SO_4^{2-} concentrations at $t = 0$ and $t = 12$ h (one-way ANOVA followed by Holm–Sidak tests, $p < 0.001$) and also significantly higher than all control incubations, including the incubations with sponge explants but without taurine at $t = 48$ h (one-way ANOVA followed by Holm–Sidak pairwise multiple comparison tests, $p < 0.001$). Two additional incubation experiments, with refined temporal resolution ($t = 0, 12, 24, 36$ and 48 h) using 1 mM and 100 μM unlabeled taurine amendments, respectively, resembled the results of the previous experiment, and displayed a significant SO_4^{2-} increase after 48 h for both taurine treatments (one-way ANOVA followed by Tukey pairwise multiple comparison tests, $p < 0.05$), with essentially a full recovery of the +100 μM taurine sulfonate in the form of SO_4^{2-} after 48 h (Fig. S7).

We observed NH_4^+ and NO_2^- production in *I. basta* incubations, with and without added unlabeled taurine (SFASW + *I. basta* + taurine; SFASW + *I. basta*), where NH_4^+ production at the end of the experiment with added taurine, drastically exceeded those of *I. basta* incubations without added taurine, consistent with the production of ammonium from taurine (Fig. 5A; $p < 0.05$, two-tailed t-test). Furthermore, a clear increase in NO_2^- production occurred within the first 12 h and was found to be significant for incubations with added taurine (Fig. 5A, SFASW + *I. basta* + taurine: one-way ANOVA followed by Tukey pairwise multiple comparison tests, $p < 0.05$). NH_4^+ and NO_2^- production in *I. basta* has previously been observed [10] and the NO_2^- production was attributed to the only ammonia-oxidizing symbiont, ‘*Ca. Nitrosospongia ianthellae*’. At the end of the experiment, NO_2^- concentrations decreased in the incubations with added taurine, consistent with the previously demonstrated inhibition of ammonia oxidation at concentrations $\geq 100 \mu\text{M}$ NH_4^+ in the *I. basta* holobiont and/or with the concomitant increased hypoxia facilitating denitrification activities [10], a capability that is encoded in ‘*Ca. Taurinisymbion ianthellae*’. Additional experiments with refined temporal resolution, displayed the same general trends (Fig. S7).

FSW incubations of the *I. basta* holobiont with ^{15}N -labeled taurine were performed. In these experiments, we were able to detect $^{15}\text{NH}_4^+$ and $^{15}\text{NO}_2^-$ formation by *I. basta* sponge explants (Fig. 5B), demonstrating taurine metabolism and oxidation of taurine-derived ammonia to nitrite by the sponge holobiont. Specifically, this indicates that the dominant thaumarchaeal symbiont hosted by *I. basta*, ‘*Ca. Nitrosospongia ianthellae*’, which was previously shown to be the only resident ammonia-oxidizer in this holobiont [10], oxidized the taurine-derived ammonia to nitrite. The amount of

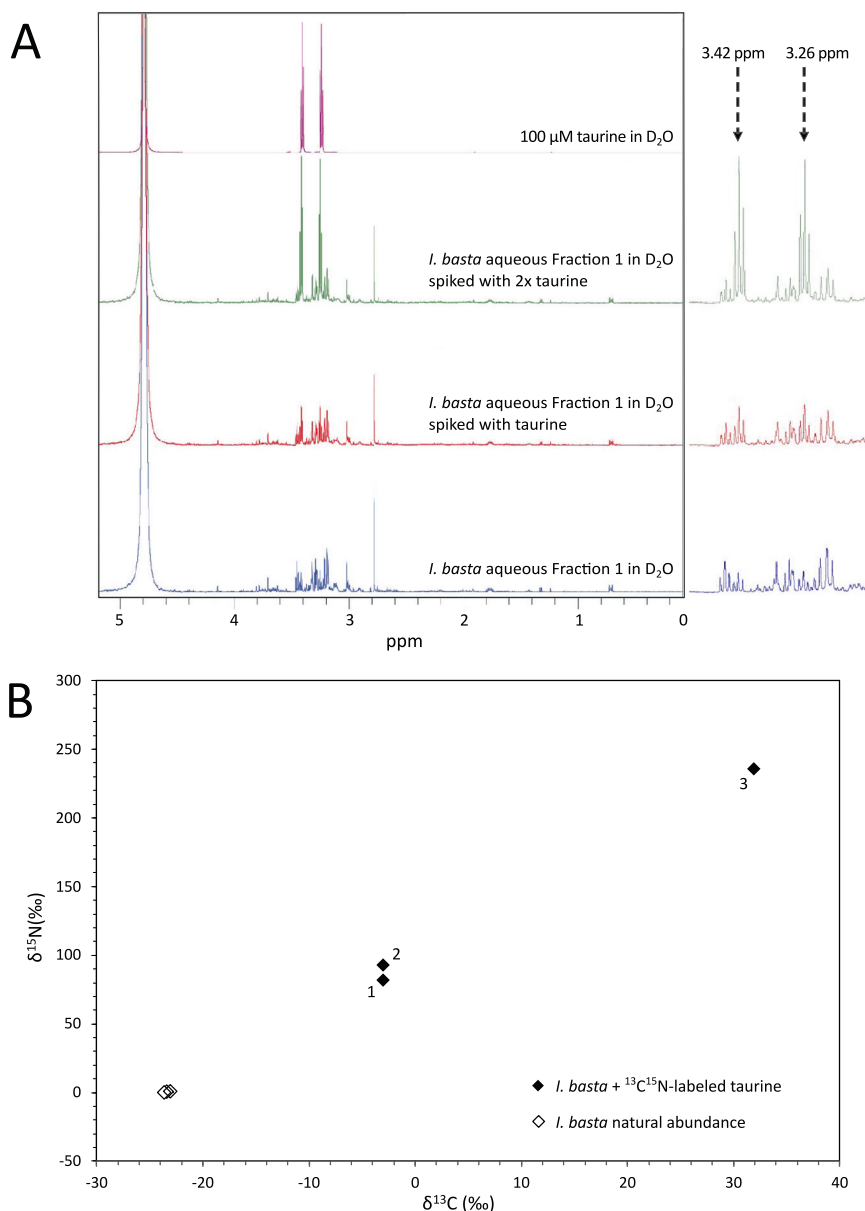


Fig. 4 Detection of taurine and incorporation of ^{13}C and ^{15}N from isotopically labeled taurine in *I. basta* holobiont biomass. **A** Detection of taurine in the aqueous fraction Fraction 1 of the 90% methanolic extract of *lanthella basta* via ^1H NMR. ^1H NMR spectra of Fraction 1 from C18 of crude methanolic extract (blue), Fraction 1 spiked with 32 μl (red) and 128 μl (green) of 100 μM taurine, as well as 100 μM taurine (purple), all acquired in D_2O . Zoomed regions are depicted of diagnostic triplet signals at 3.26 and 3.42 ppm, and the increase in taurine signal intensity with spiking. **B** Incorporation of ^{13}C - and ^{15}N -labeled taurine into sponge holobiont biomass at the total nucleic acid level as determined by EA-IRMS. Data from three sponge explants incubated with labeled taurine (numbered for reference) and three control sponge explants incubated with unlabeled taurine are depicted.

$^{15}\text{NH}_4^+$ and $^{15}\text{NO}_2^-$ derived from ^{15}N -labeled taurine in incubations with *I. basta* was always higher than the amount detected in FSW control incubations without *I. basta* at $t = 12$ and $t = 48$ h (Fig. 5B; one-way ANOVA followed by Student–Newman–Keuls pairwise multiple comparison tests, $p < 0.05$; $^{15}\text{NO}_2^-$ in FSW control incubations were undetectable in all samples). This demonstrates that these successive conversions were catalyzed by holobiont members and that this process starts as early as 12 h, suggesting that the similarly observed increase in SO_4^{2-} was also derived from taurine. In *I. basta* explant incubations without externally added taurine (FSW + *I. basta*), NH_4^+ and NO_2^- concentrations still greatly exceeded those in incubations without sponge explants and added taurine (FSW + taurine), providing additional support for the production of these compounds by *I. basta* holobiont members.

Finally, HPLC analysis of taurine concentrations for these FSW incubations confirmed uptake of taurine by the *I. basta* holobiont, since incubations with *I. basta* explants and added taurine, exhibited concentrations (FSW + *I. basta* + taurine: 1.20 ± 0.05) significantly lower than in control incubations without *I. basta* explants and added taurine (FSW + taurine: 1.73 ± 0.02 mM taurine; Kruskal–Wallis, $p < 0.05$; Fig. S8).

Taken in totality, these incubation experiments demonstrate that the *I. basta* holobiont explants actively processed and incorporated taurine-derived carbon and nitrogen, while then dissimilating the resultant ammonia moiety to nitrite and oxidizing the sulfonate moiety to sulfate, from the onset through the course of the incubations. Together with the metaproteomic dataset, we conclude that ‘*Ca. Taurinisymbion ianthellae*’ is

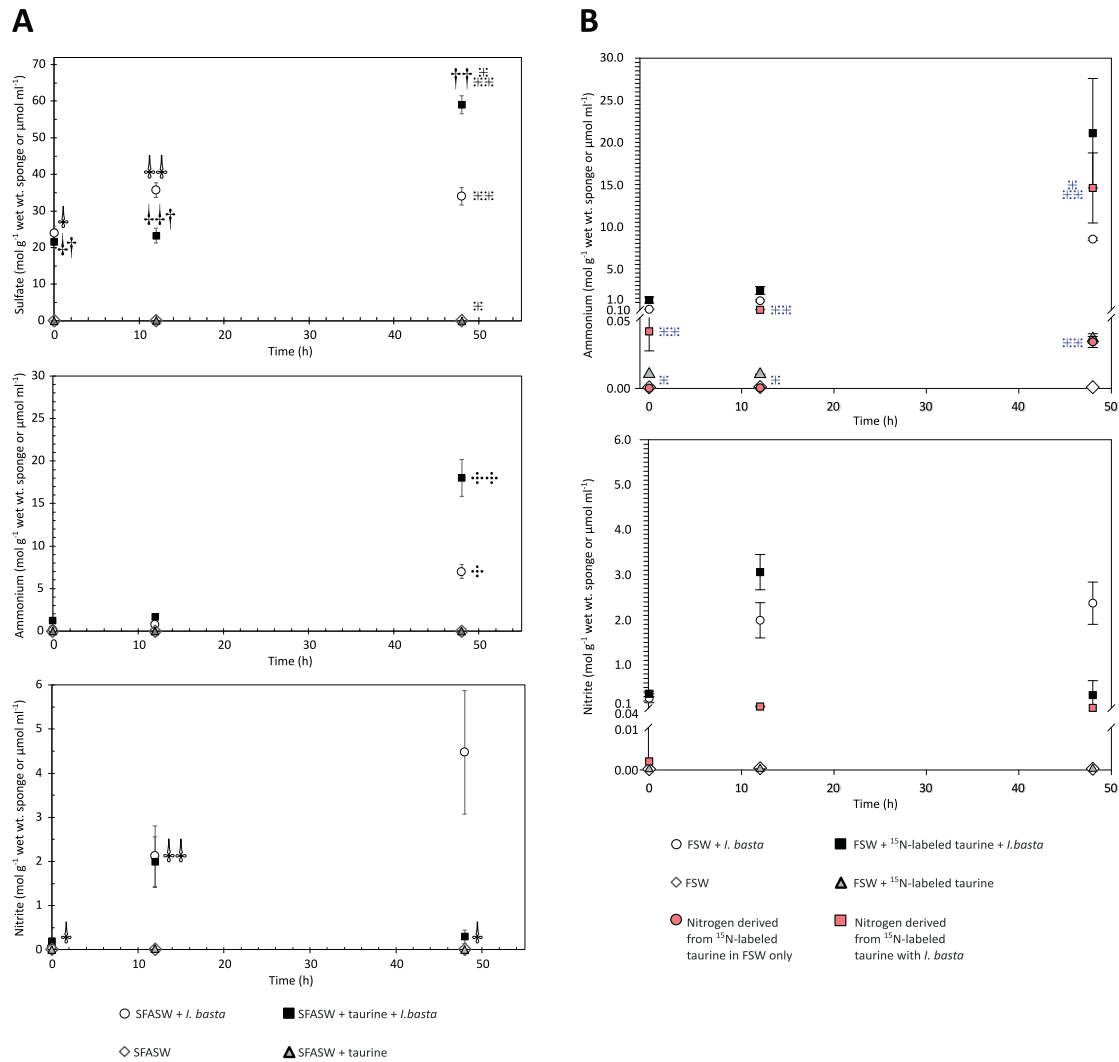


Fig. 5 Time series of dissolved sulfate, ammonium, and nitrite concentrations in incubation media of *I. basta* holobiont batch experiments. **A** 48 h incubation in sulfate-free artificial seawater (SFASW) performed either without (white circle) or with added unlabeled taurine (filled square: $t = 0$, +1 mM taurine; $t = 36$ h, +0.6 mM taurine). Concentrations are normalized to the wet weight of the respective *I. basta* explants applied in the incubations (8.83 ± 2.38 SD g sponge wet wt.; range: 6.5–13.4 g sponge wet wt.). The data from the corresponding control experiments with SFASW without *I. basta* holobiont are displayed as white diamonds (without added taurine) and gray triangles (with added taurine) and plotted on the same axes, given in $\mu\text{mol ml}^{-1}$. A starting average concentration of 0.2 mM sulfate was measured in all incubation treatments containing *I. basta* explants most likely representing residual carryover from the sponge material. Incubations were performed in biological triplicates and water samples from each incubation were taken at each time point. In **A**, $\downarrow, \downarrow, \downarrow$ symbols for sulfate concentrations denote significant difference in pairwise comparisons of incubations from $t = 0$ (\downarrow) to $t = 12$ ($\downarrow, \downarrow, \downarrow$) for both the incubations with *I. basta* and taurine and without added taurine (one-tailed t -test, $p < 0.05$); $\dagger, \dagger, \dagger$ symbols in the sulfate concentration panel reflect significant differences for sulfate concentrations for *I. basta* and taurine incubations at $t = 48$ ($\dagger, \dagger, \dagger$) when compared to the earlier time points (\dagger) (one-way ANOVA followed by Holm-Sidak tests, $p < 0.001$); similarly, the number of $\#$ symbols reflects significant differences for sulfate concentrations for incubations with *I. basta* and taurine when compared to all other treatments at $t = 48$ h (one-way ANOVA followed by Holm-Sidak tests, $p < 0.001$). \circ, \circ, \circ in the ammonium concentration panel reflects a significant difference between incubations with *I. basta* and taurine and only *I. basta* (\circ, \circ, \circ) (two-tailed t -test, $p < 0.05$). $\downarrow, \downarrow, \downarrow$ in the nitrite concentration panel reflects a significant difference between time points for the incubations with *I. basta* and taurine (one-way ANOVA followed by Tukey pairwise multiple comparison tests, $p < 0.05$). **B** Ammonium and nitrite accumulation in *I. basta* holobiont batch incubations (48 h) in natural filtered seawater (FSW) performed either with added taurine (filled symbols: $t = 0$, +1 mM taurine; $t = 36$ h, +0.6 mM taurine) or without added taurine (9.45 ± 2.53 SD g sponge wet wt.; range: 5.5–12.7 g sponge wet wt.). Taurine was added as an equimolar mixture of ¹³C- and ¹⁵N-labeled taurine to obtain sponge material for subsequent EA-IRMS and NanoSIMS analyses (by sacrificially sampling sponges at the end of the experiment) as well as to measure ¹⁵N in NH_4^+ and NO_2^- . Incubations were performed in biological triplicates and water samples from each incubation were taken at each time point. The data from the corresponding control experiments with FSW and without *I. basta* holobiont explants are displayed as white diamonds and gray triangles as in **A**. Pink symbols represent the measured concentrations of ¹⁵N in ammonium and nitrite that were a product of the added ¹⁵N-labeled taurine ($t = 0$, +0.5 mM ¹⁵N-labeled taurine; $t = 36$ h, +0.3 mM ¹⁵N-labeled taurine). The number of $\#$ symbols in the ammonium concentration panel in **B**) reflects significant differences in ¹⁵NH₄⁺ concentrations measured in incubations with *I. basta* and isotopically labeled taurine and in incubations without *I. basta* between different time points and across treatments (one-way ANOVA followed by Student-Newman-Keuls pairwise multiple comparison tests, $p < 0.05$). Error bars refer to ± 1 SE.

the holobiont member most likely responsible for this taurine incorporation and dissimilation, including the oxidation of the resultant sulfite to sulfate. Although the observed rates are potential net rates under specific incubation conditions, which will undoubtedly differ from in situ rates, as in all ex vivo experiments, the prompt incorporation and dissimilation of added exogenous taurine, suggests a N-limited sponge holobiont that is metabolically ready to access and transform this compound for anabolic as well as catabolic purposes. Recently, several laboratory and field-based studies have documented the exchange of sulfonates between marine bacteria and eukaryotic phytoplankton, with taurine (or its derivatives), always being one of the main sulfonates involved [32–34]. In co-culture, the coastal diatom *Pseudo-nitzschia multiseriis* apparently provides a *Sulfitobacter* strain (SA11) with taurine in exchange for the plant hormone indole-3-acetic acid as well as ammonium [38]. Similarly, cross-feeding between nitrite oxidizers and ammonia oxidizers has been demonstrated wherein urea or cyanate is first processed by nitrite oxidizers [118, 119], thereby providing the cleaved ammonia for oxidation to nitrite. While marine Thaumarchaeota have been shown to directly utilize urea and cyanate [120] as well as taurine exuded by mesozooplankton [121], the mechanisms for the direct utilization of these dissolved organic compounds has yet to be elucidated and indirect utilization remains a confounding factor.

A proposed model of an auxotrophy network between symbionts and the sponge host

In the *I. basta* metagenome, we found no indications for taurine biosynthesis by its microbial symbionts. Consequently, we believe it to be most likely that the taurine detected in the *I. basta* holobiont, is synthesized by the sponge, and after release, via export or sponge cell lysis, is utilized by ‘*Ca. Taurinisymbion ianthellae*’. In fact, the 5.5 $\mu\text{mol g}^{-1}$ sponge wet weight taurine, we measured in *I. basta*, would correspond to ~6.6 mM concentrations within the sponge explants used for the incubations (under the assumption that 1.2 g sponge wet wt = 1 cm^{-3} ; [97]), and we further detected taurine concentrations of 1031.05 μM (SD \pm 282.40 μM) within *I. basta* pore water. These taurine concentrations are on the high end of measured cytosolic concentrations in eukaryotic phytoplankton [34], which still does not account for further potential concentration effects in specialized cells, cell compartments, or in the mesohyl. We thus propose that endogenous taurine is either translocated by *I. basta* to ‘*Ca. Taurinisymbion ianthellae*’, as has been shown recently for DOM-derived carbon and nitrogen in a high microbial abundance (HMA) sponge [15], or is derived from host cell lysis, as a result of the rapid cell turnover characteristic of marine sponges [122, 123]. Nevertheless, it is possible that marine sponges themselves process taurine from the environment, as has been shown for bulk DOM mixtures [15, 17], instead of synthesizing it, and there remains the possibility that in our incubation experiments *I. basta* itself took up taurine and processed it. Even though our incubation experiments involved the addition of exogenous taurine, the almost immediate and continued production of the dissimilated and oxidized end products, ammonia, and sulfate, two processes for which, so far, only microbially mediated pathways have been demonstrated, suggests that the added taurine was processed primarily by the dominant gammaproteobacterial symbiont, ‘*Ca. Taurinisymbion ianthellae*’, and that it is metabolically ‘primed’ to process this compound. Alongside the incubation experimental results, as well as the measured taurine concentrations in *I. basta* bulk tissue and pore water, we therefore assume endogenous taurine supplementation by *I. basta* to be the most parsimonious route given the low taurine seawater concentrations [34, 121], competition with other microbes in seawater where taurine turnover rates are high [121], the ability of the sponge to be able to gain the taurine precursors cysteine and methionine from multiple sources (exogenous DOM and POM, as well as from its microbial symbionts), and the expression of the taurine degradation pathway by ‘*Ca. Taurinisymbion ianthellae*’ in vivo.

Taurine biosynthesis is typically considered to be a metazoan feature, but has not yet been demonstrated experimentally in sponges, nor has this capability been suggested in sequenced sponges. More recent discoveries have demonstrated bacterial and microalgal capabilities in synthesizing taurine [124, 125], and yet taurine biosynthesis in microalgae and bacteria is not universal and quite sporadic in distribution [34, 126]. Taurine biosynthesis pathways in mammalian and invertebrate tissues use cysteine as a precursor ([45] and references therein) and cysteine synthesis in metazoans requires methionine [127]. The methionine synthesis pathway, along with the biosynthesis pathways for several other essential amino acids, are generally lacking in metazoans [128–130], and thus these compounds are typically acquired via heterotrophy. While at least some sponges seem to possess the genomic repertoire for cysteine and methionine synthesis [131, 132], so far, no studies have confirmed their biosynthesis in radiolabeled amino acid precursor or feeding studies, whereas scleratinian corals can produce low amounts of methionine and perhaps even cysteine [132, 133]. ‘*Ca. Taurinisymbion ianthellae*’ encodes pathways for the synthesis of methionine and cysteine (Fig. S9), which are connected with the degradation of taurine and DMSP (Fig. 3), and also encodes several copies of EamA domain-containing proteins (IPR000620) and two copies of LeuE-type export proteins (IPR001123) (Fig. 3 and Table S5), with both families containing homologous representatives demonstrated to export cysteine [134] and methionine [135], respectively. Although further studies are needed to confirm whether marine sponges can indeed synthesize cysteine and methionine (as well as taurine), it is tempting to speculate that ‘*Ca. Taurinisymbion ianthellae*’ synthesizes and provides methionine and cysteine, either via active transport or symbiont cell lysis, to *I. basta*, and that the latter is used as a precursor for taurine biosynthesis. Cysteine or methionine auxotrophy in *I. basta* is not a precondition for this metabolic exchange to occur, as highly regulated kinetic switches may exist within the *I. basta* holobiont that is dependent on dynamic shifts in resource limitation and environmental stressors.

Although the methionine synthase (MetH)-containing pathway for methionine biosynthesis in ‘*Ca. Taurinisymbion ianthellae*’ is vitamin B₁₂ dependent (this organism also encodes a vitamin B₁₂-independent pathway using DMSP as precursor, as well as the cobalamin-independent methionine synthase, MetE; Fig. 3, Fig S9), its MAG does not contain the genes required for synthesis of this vitamin, while it does encode a putative vitamin B₁₂ transporter BtuCDF (Fig. 3 and Table S5). As the thaumarchaeal symbiont of *I. basta*, ‘*Ca. Nitrosospongia ianthellae*’, has the genomic repertoire for cobalamin (vitamin B₁₂) biosynthesis [10], it is conceivable that it provides vitamin B₁₂ for methionine biosynthesis in ‘*Ca. Taurinisymbion ianthellae*’ if DMSP is not available, while receiving ammonia dissimilated from taurine degradation. Nitrite formed by ammonia oxidation by ‘*Ca. Nitrosospongia ianthellae*’ can then serve under low oxygen concentrations as an electron acceptor in ‘*Ca. Taurinisymbion ianthellae*’. Furthermore, since nitric oxide has been shown to have an immediate contractile effect on sponges [136], and seems to be an ancient and key regulator in the marine sponge life cycle [137], the fact that ‘*Ca. Taurinisymbion ianthellae*’ encodes two denitrification genes — a nitrite reductase, *nirK* and a single subunit quinol-dependent nitric oxide reductase, *qNOR* [138] — that produces and consumes NO, suggests that this symbiont may be able to modulate host behavior. The frequent presence of an incomplete denitrification pathway along with the quinol-dependent *qNOR* — a nitrite reductase commonly found in pathogenic species [139] — in other sponge metagenomes [28], further points at the possibility that this is a widespread feature of microbial symbionts residing in marine sponges. Altogether, our data indicate a tightly connected metabolic network in the *I. basta* holobiont (Fig. 6), albeit in contrast to other selected sponges, no data are yet available for *I. basta* on the uptake of amino acids

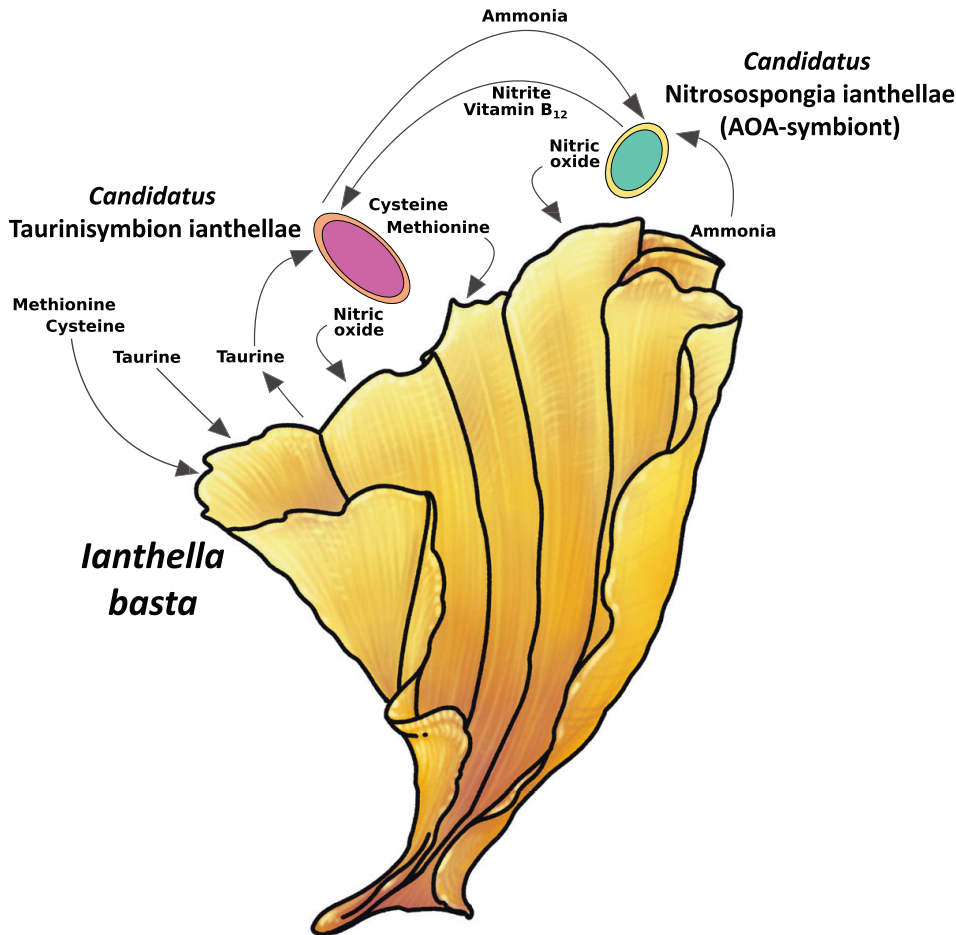


Fig. 6 Conceptual scheme of tripartite metabolic interactions within the *Ianthella basta* holobiont. A proposed metabolic network between the dominant gammaproteobacterial symbiont, '*Candidatus Taurinsymbion ianthellae*', the dominant ammonia-oxidizing thaumarchaeal symbiont, '*Candidatus Nitrosospongia ianthellae*', the marine sponge host, *Ianthella basta*, and the surrounding environment.

directly from the environment [16, 17] or from ingested free-living and symbiotic prokaryotes [140].

endogenous taurine uptake, and the numerous roles taurine may play for the functioning of these symbioses.

CONCLUSIONS

In this study, we showed through a combination of metaproteomic analyses and incubation experiments combined with isotope labeling, that the dominant *I. basta* gammaproteobacterial symbiont, '*Ca. Taurinsymbion ianthellae*', most likely uses endogenously occurring taurine that is potentially produced by the sponge holobiont, for assimilation and energy conservation. We experimentally demonstrated that the taurine dissimilation products, sulfate and ammonia, are secreted and that the latter compound is used for ammonia oxidation by the dominant thaumarchaeal symbiont — '*Ca. Nitrosospongia ianthellae*'. Taurine seems to be an important metabolite, not only in *I. basta*, but in many sponge holobiont systems, as indicated by the seeming ubiquity of taurine and taurine dissimilating genes within sponge microbiomes [25, 26, 35–37], and the appearance of a specific taurine-dissimilation/sulfite-oxidation pathway restricted mostly to symbiotic microorganisms [25, 26, 109]. Taurine also appears to be a central metabolite in several other metazoan holobiont systems such as in cnidarians, various bivalve species [44, 45, 141, 142], and in mammalian gut systems [39, 40]. Future research is needed to further disentangle the mechanisms of taurine synthesis via symbiont-derived or environmentally supplied precursors in marine sponge holobionts, to better understand the role of exogenous and

DATA AVAILABILITY

The metagenomic raw reads are available in the European Nucleotide Archive under BioProject accession number PRJEB9378. The MAG for '*Ca. Taurinsymbion ianthellae*' was assembled from run ERR884062 and is available under the accession number ERS14904192. The proteomics raw data have been deposited to the ProteomeX-change Consortium via the PRIDE partner repository with the dataset identifier PXD012484 and 10.6019/PXD012484.

REFERENCES

- Bell JJ. The functional roles of marine sponges. *Estuar Coast Shelf Sci.* 2008;79:341–53.
- de Goeij J, van den Berg H, van Oostveen M, Epping E, van Duyl F. Major bulk dissolved organic carbon (DOC) removal by encrusting coral reef cavity sponges. *Mar Ecol Prog Ser.* 2008;357:139–51.
- de Goeij JM, van Oevelen D, Vermeij MJA, Osinga R, Middelburg JJ, de Goeij AFP, et al. Surviving in a marine desert: the sponge loop retains resources within coral reefs. *Science.* 2013;342:108–10.
- Rix L, de Goeij JM, Mueller CE, Struck U, Middelburg JJ, van Duyl FC, et al. Coral mucus fuels the sponge loop in warm- and cold-water coral reef ecosystems. *Sci Rep.* 2016;6:1–11.
- Webster NS, Thomas T. The sponge hologenome. *mBio.* 2016;7:e00135–16.
- Zhang F, Jonas L, Lin H, Hill RT. Microbially mediated nutrient cycles in marine sponges. *FEMS Microbiol Ecol.* 2019;95:115.
- Wilkinson CR. Net Primary productivity in coral reef sponges. *Science.* 1983;219:410–2.

8. Wilkinson CR, Fay P. Nitrogen fixation in coral reef sponges with symbiotic cyanobacteria. *Nature*. 1979;279:527–9.
9. Bayer K, Schmitt S, Hentschel U. Physiology, phylogeny and in situ evidence for bacterial and archaeal nitrifiers in the marine sponge *Aplysina aerophoba*. *Environ Microbiol*. 2008;10:2942–55.
10. Moeller FU, Webster NS, Herbold CW, Behnam F, Domman D, Albertsen M, et al. Characterization of a thaumarchaeal symbiont that drives incomplete nitrification in the tropical sponge *lanthella basta*. *Environ Microbiol*. 2019;21:3831–54.
11. Hoffmann F, Larsen O, Thiel V, Rapp HT, Pape T, Michaelis W, et al. An anaerobic world in sponges. *Geomicrobiol J*. 2005;22:1–10.
12. Hoffmann F, Radax R, Woebken D, Holtappels M, Lavik G, Rapp HT, et al. Complex nitrogen cycling in the sponge *Geodia barretti*. *Environ Microbiol*. 2009;11:2228–43.
13. Freeman CJ, Thacker RW. Complex interactions between marine sponges and their symbiotic microbial communities. *Limnol Oceanogr*. 2011;56:1577–86.
14. Freeman CJ, Thacker RW, Baker DM, Fogel ML. Quality or quantity: is nutrient transfer driven more by symbiont identity and productivity than by symbiont abundance? *ISME J*. 2013;7:1116–25.
15. Hudspeth M, Rix L, Achlatis M, Bougouffar J, Guagliardo P, Clode PL, et al. Subcellular view of host–microbiome nutrient exchange in sponges: insights into the ecological success of an early metazoan–microbe symbiosis. *Microbiome*. 2021;9:1–15.
16. Achlatis M, Pernice M, Green K, de Goeij JM, Guagliardo P, Kilburn MR, et al. Single-cell visualization indicates direct role of sponge host in uptake of dissolved organic matter. *Proc R Soc B Biol Sci*. 2019;286:20192153.
17. Rix L, Ribes M, Coma R, Jahn MT, de Goeij JM, van Oevelen D, et al. Heterotrophy in the earliest gut: a single-cell view of heterotrophic carbon and nitrogen assimilation in sponge–microbe symbioses. *ISME J*. 2020;14:2554–67.
18. Taylor MW, Radax R, Steger D, Wagner M. Sponge-associated microorganisms: evolution, ecology, and biotechnological potential. *Microbiol Mol Biol Rev*. 2007;71:295–347.
19. Webster NS, Taylor MW. Marine sponges and their microbial symbionts: love and other relationships: Marine sponge microbiology. *Environ Microbiol*. 2012;14:335–46.
20. Thomas T, Moitinho-Silva L, Lurgi M, Björk JR, Easson C, Astudillo-García C, et al. Diversity, structure and convergent evolution of the global sponge microbiome. *Nat Commun*. 2016;7:11870.
21. Siegl A, Kamke J, Hochmuth T, Piel J, Richter M, Liang C, et al. Single-cell genomics reveals the lifestyle of Poribacteria, a candidate phylum symbiotically associated with marine sponges. *ISME J*. 2011;5:61–70.
22. Moitinho-Silva L, Diez-Vives C, Batani G, Esteves AI, Jahn MT, Thomas T. Integrated metabolism in sponge–microbe symbiosis revealed by genome-centered metatranscriptomics. *ISME J*. 2017;11:1651–66.
23. Fiore CL, Labrie M, Jarett JK, Lesser MP. Transcriptional activity of the giant barrel sponge, *Xestospongia muta* Holobiont: molecular evidence for metabolic interchange. *Front Microbiol*. 2015;6:364.
24. Moreno-Pino M, Cristi A, Gillooly JF, Trefault N. Characterizing the microbiomes of Antarctic sponges: a functional metagenomic approach. *Sci Rep*. 2020;10:645.
25. Tian R-M, Wang Y, Bougouffar S, Gao Z-M, Cai L, Bajic V, et al. Genomic analysis reveals versatile heterotrophic capacity of a potentially symbiotic sulfur-oxidizing bacterium in sponge. *Environ Microbiol*. 2014;16:3548–61.
26. Gauthier M-EA, Watson JR, Degnan SM. Draft genomes shed light on the dual bacterial symbiosis that dominates the microbiome of the coral reef sponge amphimedon queenslandica. *Front Mar Sci*. 2016;3:196.
27. Hallam SJ, Konstantinidis KT, Putnam N, Schleper C, Watanabe Y-I, Sugahara J, et al. Genomic analysis of the uncultivated marine crenarchaeote *Cenarchaeum symbiosum*. *Proc Natl Acad Sci USA*. 2006;103:18296–301.
28. Fan L, Reynolds D, Liu M, Stark M, Kjelleberg S, Webster NS, et al. Functional equivalence and evolutionary convergence in complex communities of microbial sponge symbionts. *Proc Natl Acad Sci USA*. 2012;109:E1878–87.
29. Hentschel U, Piel J, Degnan SM, Taylor MW. Genomic insights into the marine sponge microbiome. *Nat Rev Microbiol*. 2012;10:641–54.
30. Liu M, Fan L, Zhong L, Kjelleberg S, Thomas T. Metaproteomic analysis of a community of sponge symbionts. *ISME J*. 2012;6:1515–25.
31. Hooper JNA, Capon RJ, Keenan CP, Parry DL, Smit N. Chemotaxonomy of marine sponges: families microcionidae, raspaillidae and axinellidae, and their relationships with other families in the orders poecilosclerida and axinellida (Porifera: Demospongiae). *Invert Syst*. 1992;6:261–301.
32. Durham BP, Sharma S, Luo H, Smith CB, Amin SA, Bender SJ, et al. Cryptic carbon and sulfur cycling between surface ocean plankton. *Proc Natl Acad Sci USA*. 2015;112:453–7.
33. Landa M, Burns AS, Roth SJ, Moran MA. Bacterial transcriptome remodeling during sequential co-culture with a marine dinoflagellate and diatom. *ISME J*. 2017;11:2677–90.
34. Durham BP, Boysen AK, Carlson LT, Groussman RD, Heal KR, Cain KR, et al. Sulfonate-based networks between eukaryotic phytoplankton and heterotrophic bacteria in the surface ocean. *Nat Microbiol*. 2019;4:1706–15.
35. Karimi E, Keller-Costa T, Slaby BM, Cox CJ, da Rocha UN, Hentschel U, et al. Genomic blueprints of sponge-prokaryote symbiosis are shared by low abundant and cultivatable Alphaproteobacteria. *Sci Rep*. 2019;9:1999.
36. Botté ES, Nielsen S, Abdul Wahab MA, Webster J, Robbins S, Thomas T, et al. Changes in the metabolic potential of the sponge microbiome under ocean acidification. *Nat Commun*. 2019;10:4134.
37. Engelberts JP, Robbins SJ, de Goeij JM, Aranda M, Bell SC, Webster NS. Characterization of a sponge microbiome using an integrative genome-centric approach. *ISME J*. 2020;14:1100–10.
38. Amin SA, Hmelo LR, van Tol HM, Durham BP, Carlson LT, Heal KR, et al. Interaction and signalling between a cosmopolitan phytoplankton and associated bacteria. *Nature*. 2015;522:98–101.
39. Stacy A, Andrade-Oliveira V, McCulloch JA, Hild B, Oh JH, Perez-Chaparro PJ, et al. Infection trains the host for microbiota-enhanced resistance to pathogens. *Cell*. 2021;184:615–e17.
40. Ye H, Borusak S, Eberl C, Hanson BT, Zwirzitz B, Herbold CW, et al. A novel taurine-respiring murine gut bacterium contributes to colonization resistance against enteropathogens. *bioRxiv*. <https://doi.org/10.1101/2022.10.05.510937> (2022)
41. Atlas M, Bahl JJ, Roeske W, Bressler R. In vitro osmoregulation of taurine in fetal mouse hearts. *J Mol Cell Cardiol*. 1984;16:311–20.
42. Schaffer S, Takahashi K, Azuma J. Role of osmoregulation in the actions of taurine. *Amino Acids*. 2000;19:527–46.
43. Huxtable RJ. Physiological actions of taurine. *Physiol Rev*. 1992;72:101–63.
44. Lee R, Childress J, Desaulniers N. The effects of exposure to ammonia on ammonia and taurine pools of the symbiotic clam. *J Exp Biol*. 1997;200:2797–805.
45. Joyner JL, Peyer SM, Lee RW. Possible roles of sulfur-containing amino acids in a chemosynthetic bacterium–mollusc symbiosis. *Biol Bull*. 2003;205:331–8.
46. Alberic P, Boulegue J. Unusual amino compounds in the tissues of *Calyptogena phaseoliformis* (Japan Trench): possible link to symbiosis. *Prog Oceanogr*. 1990;24:89–101.
47. Conway NM, Howes BL, McDowell Capuzzo JE, Turner RD, Cavanaugh CM. Characterization and site description of *Solemya borealis* (Bivalvia; Solemyidae), another bivalve–bacteria symbiosis. *Mar Biol*. 1992;112:601–13.
48. Conway NM, McDowell Capuzzo JE. High taurine levels in the *Solemya velum* symbiosis. *Comp Biochem Physiol B*. 1992;102:175–85.
49. Pranal V, Fiala-Médioni A, Colomines J. Amino acid and related compound composition in two symbiotic mytilid species from hydrothermal vents. *Mar Ecol Prog Ser*. 1995;119:155–66.
50. Pruski AM, Fiala-Médioni A, Boulegue J, Colomines JC. Sulphur metabolism in chemosynthetic symbiont-containing invertebrates from hydrothermal vents. *Cah Biol Mar*. 1997;2:135–6.
51. Pallas PS. *Elenchus zoophytorum* sistens generum adumbrationes generales et specierum cognitarum succinctas descriptiones, cum selectis auctorum synonymis. Hagae-Comitum, Apud Petrum van Cleef. 1766;379. <https://doi.org/10.5962/bhl.title.6595>.
52. Bergquist PR, Kelly-Borges M. Systematics and biogeography of the genus *lanthella* (Demospongiae: Verongida: lanthellidae) in the south-west Pacific. *Beagle Rec Mus Art Galleries North Territory*. 1995;12:151.
53. Hentschel U, Usher KM, Taylor MW. Marine sponges as microbial fermenters. *FEMS Microbiol Ecol*. 2006;55:167–77.
54. Webster NS, Taylor MW, Behnam F, Lückner S, Rattei T, Whalan S, et al. Deep sequencing reveals exceptional diversity and modes of transmission for bacterial sponge symbionts. *Environ Microbiol*. 2010;12:2070–82.
55. Luter HM, Whalan S, Webster NS. Exploring the role of microorganisms in the disease-like syndrome affecting the sponge *lanthella basta*. *Appl Environ Microbiol*. 2010;76:5736–44.
56. Freckleton ML, Luter HM, Andreakis N, Webster NS, Motti CA. Qualitative variation in colour morphotypes of *lanthella basta* (Porifera: Verongida). *Hydrobiologia*. 2012;687:191–203.
57. Luter HM, Whalan S, Webster NS. Thermal and sedimentation stress are unlikely causes of brown spot syndrome in the coral reef sponge, *lanthella basta*. *PLoS One*. 2012;7:e39779.
58. Williams TJ, Long E, Evans F, DeMaere MZ, Lauro FM, Raftery MJ, et al. A metaproteomic assessment of winter and summer bacterioplankton from Antarctic Peninsula coastal surface waters. *ISME J*. 2012;6:1883–1900.
59. Strehlow BW, Pineda M-C, Duckworth A, Kendrick GA, Renton M, Wahab MAA, et al. Sediment tolerance mechanisms identified in sponges using advanced imaging techniques. *PeerJ*. 2017;5:e3904.
60. Lu X, Zou L, Clevinger C, Liu Q, Hollibaugh JT, Mou X. Temporal dynamics and depth variations of dissolved free amino acids and polyamines in coastal seawater determined by high-performance liquid chromatography. *Mar Chem*. 2014;163:36–44.
61. Bankevich A, Nurk S, Antipov D, Gurevich AA, Dvorkin M, Kulikov AS, et al. SPAdes: a new genome assembly algorithm and its applications to single-cell sequencing. *J Comput Biol*. 2012;19:455–77.

62. Kang DD, Froula J, Egan R, Wang Z. MetaBAT, an efficient tool for accurately reconstructing single genomes from complex microbial communities. *PeerJ*. 2015;3:e1165.
63. Olm MR, Brown CT, Brooks B, Banfield JF. dRep: a tool for fast and accurate genomic comparisons that enables improved genome recovery from metagenomes through de-replication. *ISME J*. 2017;11:2864–8.
64. Parks DH, Imelfort M, Skennerton CT, Hugenholtz P, Tyson GW. CheckM: assessing the quality of microbial genomes recovered from isolates, single cells, and metagenomes. *Genome Res*. 2015;25:1043–55.
65. Vallenet D, Engelen S, Mornico D, Cruveiller S, Fleury L, Lajus A, et al. MicroScope: a platform for microbial genome annotation and comparative genomics. *Database (Oxf)*. 2009;2009:bap021.
66. Zhang S, Song W, Wemheuer B, Reveillaud J, Webster N, Thomas T. Comparative genomics reveals ecological and evolutionary insights into sponge-associated *Thaumarchaeota*. *mSystems*. 2019;4:e00288–19.
67. Stoecker K, Dorninger C, Daims H, Wagner M. Double labeling of oligonucleotide probes for fluorescence in situ hybridization (DOPE-FISH) improves signal intensity and increases rRNA accessibility. *Appl Environ Microbiol*. 2010;76:922–6.
68. Daims H, Brühl A, Amann R, Schleifer K-H, Wagner M. The domain-specific probe EUB338 is insufficient for the detection of all bacteria: development and evaluation of a more comprehensive probe set. *Syst Appl Microbiol*. 1999;22:434–44.
69. Wallner G, Amann R, Beisler W. Optimizing fluorescent in situ hybridization with rRNA-targeted oligonucleotide probes for flow cytometric identification of microorganisms. *Cytometry*. 1993;14:136–43.
70. Simister RL, Deines P, Botté ES, Webster NS, Taylor MW. Sponge-specific clusters revisited: a comprehensive phylogeny of sponge-associated microorganisms: Sponge-associated microorganisms. *Environ Microbiol*. 2012;14:517–24.
71. Nguyen L-T, Schmidt HA, von Haeseler A, Minh BQ. IQ-TREE: a fast and effective stochastic algorithm for estimating maximum-likelihood phylogenies. *Mol Biol Evol*. 2015;32:268–74.
72. Kalyaanamoorthy S, Minh BQ, Wong TKF, von Haeseler A, Jermini LS. ModelFinder: fast model selection for accurate phylogenetic estimates. *Nat Methods*. 2017;14:587–9.
73. Hoang DT, Chernomor O, von Haeseler A, Minh BQ, Vinh LS. UFBoot2: improving the ultrafast bootstrap approximation. *Mol Biol Evol*. 2018;35:518–22.
74. Lagkouvardos I, Joseph D, Kapfhammer M, Giritli S, Horn M, Haller D, et al. IMGs: a comprehensive open resource of processed 16S rRNA microbial profiles for ecology and diversity studies. *Sci Rep*. 2016;6:33721.
75. Berger SA, Krompass D, Stamatakis A. Performance, accuracy, and web server for evolutionary placement of short sequence reads under maximum likelihood. *Syst Biol*. 2011;60:291–302.
76. Stamatakis A. RAxML version 8: a tool for phylogenetic analysis and post-analysis of large phylogenies. *Bioinformatics*. 2014;30:1312–3.
77. Otto A, Bernhardt J, Meyer H, Schaffer M, Herbst F-A, Siebourg J, et al. Systems-wide temporal proteomic profiling in glucose-starved *Bacillus subtilis*. *Nat Commun*. 2010;1:137.
78. Verberkmoes NC, Russell AL, Shah M, Godzik A, Rosenquist M, Halfvarson J, et al. Shotgun metaproteomics of the human distal gut microbiota. *ISME J*. 2009;3:179–89.
79. Heinz E, Williams TA, Nakjang S, Noël CJ, Swan DC, Goldberg AV, et al. The genome of the obligate intracellular parasite *Trachipleistophora hominis*: new insights into microsporidian genome dynamics and reductive evolution. *PLoS Pathog*. 2012;8:e1002979.
80. Peng J, Elias JE, Thoreen CC, Licklider LJ, Gygi SP. Evaluation of multidimensional chromatography coupled with tandem mass spectrometry (LC/LC – MS/MS) for large-scale protein analysis: the yeast proteome. *J Proteome Res*. 2003;2:43–50.
81. Elias JE, Gygi SP. Target-decoy search strategy for increased confidence in large-scale protein identifications by mass spectrometry. *Nat Methods*. 2007;4:207–14.
82. Florens L, Carozza M, Swanson S, Fournier M, Coleman M, Workman J, et al. Analyzing chromatin remodeling complexes using shotgun proteomics and normalized spectral abundance factors. *Methods*. 2006;40:303–11.
83. Tapiolas DM, Raina J-B, Lutz A, Willis BL, Motti CA. Direct measurement of dimethylsulfoniopropionate (DMSP) in reef-building corals using quantitative nuclear magnetic resonance (qNMR) spectroscopy. *J Exp Mar Biol Ecol*. 2013;443:85–89.
84. Salas E, Gorfer M, Bandian D, Wang B, Kaiser C, Wanek W. A rapid and sensitive assay to quantify amino sugars, neutral sugars and uronic acid necromass biomarkers using pre-column derivatization, ultra-high-performance liquid chromatography and high-resolution mass spectrometry. *Soil Biol Biochem*. 2023;177:108927.
85. Angel R, Claus P, Conrad R. Methanogenic archaea are globally ubiquitous in aerated soils and become active under wet anoxic conditions. *ISME J*. 2012;6:847–62.
86. Fry B. Stable isotope ecology. New York, NY 10013, USA: Springer Science +Business Media, LLC; (2006).
87. Sørensen P, Jensen ES. Sequential diffusion of ammonium and nitrate from soil extracts to a polytetrafluoroethylene trap for 15 N determination. *Anal Chim Acta*. 1991;252:201–3.
88. Lachouani P, Frank AH, Wanek W. A suite of sensitive chemical methods to determine the $\delta^{15}\text{N}$ of ammonium, nitrate and total dissolved N in soil extracts. *Rapid Commun Mass Spectrom*. 2010;24:3615–23.
89. Tian R-M, Sun J, Cai L, Zhang W-P, Zhou G-W, Qiu J-W, et al. The deep-sea glass sponge *Lophophysema eversa* harbours potential symbionts responsible for the nutrient conversions of carbon, nitrogen and sulfur: Potential symbionts in a glass sponge. *Environ Microbiol*. 2016;18:2481–94.
90. Parks DH, Chuvochina M, Waite DW, Rinke C, Skarshewski A, Chaumeil P-A, et al. A standardized bacterial taxonomy based on genome phylogeny substantially revises the tree of life. *Nat Biotechnol*. 2018;36:996–1004.
91. Reveillaud J, Maignien L, Eren AM, Huber JA, Apprill A, Sogin ML, et al. Host-specificity among abundant and rare taxa in the sponge microbiome. *ISME J*. 2014;8:1198–209.
92. Rust M, Helfrich EJM, Freeman MF, Nanudorn P, Field CM, Rückert C, et al. A multiproducer microbiome generates chemical diversity in the marine sponge *Mycale hentscheli*. *Proc Natl Acad Sci USA*. 2020;117:9508–18.
93. Storey MA, Andreassend SK, Bracegirdle J, Brown A, Keyzers RA, Ackerley DF, et al. Metagenomic exploration of the marine sponge *Mycale hentscheli* uncovers multiple polyketide-producing bacterial symbionts. *mBio*. 2020;11:e02997–19.
94. Glasl B, Robbins S, Frade PR, Marangon E, Laffy PW, Bourne DG, et al. Comparative genome-centric analysis reveals seasonal variation in the function of coral reef microbiomes. *ISME J*. 2020;14:1435–50.
95. Luo C, Rodriguez-R LM, Konstantinidis KT. MyTaxa: an advanced taxonomic classifier for genomic and metagenomic sequences. *Nucleic Acids Res*. 2014;42:e73–e73.
96. Konstantinidis KT, Rosselló-Móra R, Amann R. Uncultivated microbes in need of their own taxonomy. *ISME J*. 2017;11:2399–406.
97. Schläppy M-L, Schöttner SI, Lavik G, Kuypers MMM, de Beer D, Hoffmann F. Evidence of nitrification and denitrification in high and low microbial abundance sponges. *Mar Biol*. 2010;157:593–602.
98. Cook AM, Denger K. Metabolism of Taurine in Microorganisms: a primer in molecular biodiversity? *Adv Exp Med Biol*. 2006;583:3–13.
99. Grein F, Ramos AR, Venceslau SS, Pereira IAC. Unifying concepts in anaerobic respiration: Insights from dissimilatory sulfur metabolism. *Biochim Biophys Acta Bioenerg*. 2013;1827:145–60.
100. Rein U, Gueta R, Denger K, Ruff J, Hollemeyer K, Cook AM. Dissimilation of cysteate via 3-sulfolactate sulfo-lyase and a sulfate exporter in *Paracoccus pantotrophus* NKNCYSA. *Microbiology*. 2005;151:737–47.
101. Kertesz MA. Riding the sulfur cycle – metabolism of sulfonates and sulfate esters in Gram-negative bacteria. *FEMS Microbiol Rev*. 2000;24:135–75.
102. Elser JJ, Bracken MES, Cleland EE, Gruner DS, Harpole WS, Hillebrand H, et al. Global analysis of nitrogen and phosphorus limitation of primary producers in freshwater, marine and terrestrial ecosystems. *Ecol Lett*. 2007;10:1135–42.
103. Reese AT, Pereira FC, Schintlmeyer A, Berry D, Wagner M, Hale LP, et al. Microbial nitrogen limitation in the mammalian large intestine. *Nat Microbiol*. 2018;3:1441–50.
104. Kleiner M, Wentrup C, Lott C, Teeling H, Wetzels S, Young J, et al. Metaproteomics of a gutless marine worm and its symbiotic microbial community reveal unusual pathways for carbon and energy use. *Proc Natl Acad Sci USA*. 2012;109:E1173–182.
105. Lackner G, Peters EE, Helfrich EJM, Piel J. Insights into the lifestyle of uncultured bacterial natural product factories associated with marine sponges. *Proc Natl Acad Sci USA*. 2017;114:E347–56.
106. Engelberts JP, Robbins SJ, Herbold CW, Moeller FU, Jehmlich N, Laffy PW, et al. Metabolic reconstruction of the near complete microbiome of the model sponge *lanthella basta*. *Environ Microbiol*. 2022;1462–2920:16302.
107. Baldock MI, Denger K, Smits THM, Cook AM. *Roseovarius* sp. strain 217: aerobic taurine dissimilation via acetate kinase and acetate-CoA ligase. *FEMS Microbiol Lett*. 2007;271:202–6.
108. Lehmann S. Sulfite dehydrogenases in organotrophic bacteria: enzymes, genes and regulation. Konstanz, Germany: University of Konstanz; 2013.
109. Woyke T, Teeling H, Ivanova NN, Huntemann M, Richter M, Gloeckner FO, et al. Symbiosis insights through metagenomic analysis of a microbial consortium. *Nature*. 2006;443:950–5.
110. Schwalbach MS, Tripp HJ, Steindler L, Smith DP, Giovannoni SJ. The presence of the glycolysis operon in SAR11 genomes is positively correlated with ocean productivity. *Environ Microbiol*. 2010;12:490–500.
111. Steindler L, Schwalbach MS, Smith DP, Chan F, Giovannoni SJ. Energy starved candidatus *Pelagibacter ubique* substitutes light-mediated ATP production for endogenous carbon respiration. *PLoS One*. 2011;6:e19725.

112. Gamagedara S, Shi H, Ma Y. Quantitative determination of taurine and related biomarkers in urine by liquid chromatography–tandem mass spectrometry. *Anal Bioanal Chem.* 2012;402:763–70.
113. Shinagawa A, Suzuki T, Konosu S. The role of free amino acids and betaines in intracellular osmoregulation of marine sponges. *Nippon Suisan Gakkaishi.* 1992;58:1717–22.
114. Engelberts JP, Abdul Wahab MA, Maldonado M, Rix L, Marangon E, Robbins SJ, et al. Microbes from mum: symbiont transmission in the tropical reef sponge *lanthella basta*. *ISME Commun.* 2022;2:90.
115. Brüggemann C, Denger K, Cook AM, Ruff J. Enzymes and genes of taurine and isethionate dissimilation in *Paracoccus denitrificans*. *Microbiology.* 2004;150:805–16.
116. Weinitschke S, von Rekowski KS, Denger K, Cook AM. Sulfoacetaldehyde is excreted quantitatively by *Acinetobacter calcoaceticus* SW1 during growth with taurine as sole source of nitrogen. *Microbiology.* 2005;151:1285–90.
117. Denger K, Smits THM, Cook AM. Genome-enabled analysis of the utilization of taurine as sole source of carbon or of nitrogen by *Rhodobacter sphaeroides* 2.4.1. *Microbiology.* 2006;152:3197–206.
118. Palatinszky M, Herbold C, Jehmlich N, Pogoda M, Han P, von Bergen M, et al. Cyanate as an energy source for nitrifiers. *Nature.* 2015;524:105–8.
119. Koch H, Lückner S, Albertsen M, Kitzinger K, Herbold C, Spieck E, et al. Expanded metabolic versatility of ubiquitous nitrite-oxidizing bacteria from the genus *Nitrospira*. *Proc Natl Acad Sci USA.* 2015;112:11371–6.
120. Kitzinger K, Padilla CC, Marchant HK, Hach PF, Herbold CW, Kidane AT, et al. Cyanate and urea are substrates for nitrification by Thaumarchaeota in the marine environment. *Nat Microbiol.* 2019;4:234–43.
121. Clifford EL, De Corte D, Amano C, Paliaga P, Ivančić I, Ortiz V, et al. Mesozooplankton taurine production and prokaryotic uptake in the northern Adriatic Sea. *Limnol Oceanogr.* 2020;65:2730–47.
122. De Goeij JM, De Kluijver A, Van Duyl FC, Vacelet J, Wijffels RH, De Goeij AFPM, et al. Cell kinetics of the marine sponge *Halisarca caerulea* reveal rapid cell turnover and shedding. *J Exp Biol.* 2009;212:3892–3900.
123. Alexander BE, Liebrand K, Osinga R, van der Geest HG, Admiraal W, Cleutjens JPM, et al. Cell turnover and detritus production in marine sponges from tropical and temperate benthic ecosystems. *PLoS One.* 2014;9:e109486.
124. Agnello G, Chang LL, Lamb CM, Georgiou G, Stone EM. Discovery of a substrate selectivity motif in amino acid decarboxylases unveils a taurine biosynthesis pathway in prokaryotes. *ACS Chem Biol.* 2013;8:2264–71.
125. Tevatia R, Allen J, Rudrappa D, White D, Clemente TE, Cerutti H, et al. The taurine biosynthetic pathway of microalgae. *Algal Res.* 2015;9:21–26.
126. Moran MA, Durham BP. Sulfur metabolites in the pelagic ocean. *Nat Rev Microbiol.* 2019;17:665–78.
127. Wybouw N, Dermauw W, Tirry L, Stevens C, Grbić M, Feyereisen R, et al. A gene horizontally transferred from bacteria protects arthropods from host plant cyanide poisoning. *eLife.* 2014;3:e02365.
128. Guedes R, Prosdocimi F, Fernandes G, Moura L, Ribeiro H, Ortega J. Amino acids biosynthesis and nitrogen assimilation pathways: a great genomic deletion during eukaryotes evolution. *BMC Genom.* 2011;12:52.
129. Costa I, Thompson J, Ortega J, Prosdocimi F. Metazoan remaining genes for essential amino acid biosynthesis: sequence conservation and evolutionary analyses. *Nutrients.* 2014;7:1–16.
130. Richter DJ, Fozouni P, Eisen MB, King N. Gene family innovation, conservation and loss on the animal stem lineage. *eLife.* 2018;7:e34226.
131. Munroe S, Sandoval K, Martens DE, Sipkema D, Pomponi SA. Genetic algorithm as an optimization tool for the development of sponge cell culture media. *Vitr Cell Dev Biol Anim.* 2019;55:149–58.
132. Salazar OR N, Arun P, Cui G, Bay LK, van Oppen MJH, Webster NS, et al. The coral *Acropora loripes* genome reveals an alternative pathway for cysteine biosynthesis in animals. *Sci Adv.* 2022;8:eabq0304.
133. Fitzgerald LM, Szmant AM. Biosynthesis of 'essential' amino acids by scleractinian corals. *Biochem.* 1997;322:213–21.
134. Dassler T, Maier T, Winterhalter C, Bock A. Identification of a major facilitator protein from *Escherichia coli* involved in efflux of metabolites of the cysteine pathway. *Mol Microbiol.* 2000;36:1101–12.
135. Kutukova EA, Livshits VA, Altman IP, Ptitsyn LR, Ziyatdinov MH, Tokmakova IL, et al. The *yeaS* (*leuE*) gene of *Escherichia coli* encodes an exporter of leucine, and the *Lrp* protein regulates its expression. *FEBS Lett.* 2005;579:4629–34.
136. Elliott GRD, Leys SP. Evidence for glutamate, GABA and NO in coordinating behaviour in the sponge, *Ephydatia muelleri* (Demospongiae, Spongillidae). *J Exp Biol.* 2010;213:2310–21.
137. Ueda N, Richards GS, Degnan BM, Kranz A, Adamska M, Croll RP, et al. An ancient role for nitric oxide in regulating the animal pelagobenthic life cycle: evidence from a marine sponge. *Sci Rep.* 2016;6:37546.
138. Cramm R, Pohlmann A, Friedrich B. Purification and characterization of the single-component nitric oxide reductase from *Ralstonia eutropha* H16. *FEBS Lett.* 1999;460:6–10.
139. Hendriks J, Oubrie A, Castresana J, Urbani A, Gemeinhardt S, Saraste M. Nitric oxide reductases in bacteria. *Biochim Biophys Acta Bioenerg.* 2000;1459:266–73.
140. Leys SP, Kahn AS, Fang JKH, Kutti T, Bannister RJ. Phagocytosis of microbial symbionts balances the carbon and nitrogen budget for the deep-water boreal sponge *Geodia barretti*. *Limnol Oceanogr.* 2018;63:187–202.
141. Deane EM, O'Brien RW. Uptake of sulphate, taurine, cysteine and methionine by symbiotic and free-living dinoflagellates. *Arch Microbiol.* 1981;128:311–9.
142. Wang JT, Douglas AE. Nutrients, signals, and photosynthate release by symbiotic algae (the impact of taurine on the dinoflagellate alga symbiodinium from the sea anemone *Aiptasia pulchella*). *Plant Physiol.* 1997;114:631–6.

ACKNOWLEDGEMENTS

We thank Emmanuelle Botte for assisting with experimental incubations, Heidi Luter for assisting with field collections and Pam Engelberts for helpful discussions. We are grateful to Erika Kristel Salas Hernández and Wolfgang Wanek for their support with the UPLC taurine measurements. We thank Bernhard Schink for valuable advice regarding the provisional naming of the gammaproteobacterial symbiont.

AUTHOR CONTRIBUTIONS

FUM, NSW, AR, and M. Wagner conceived and developed the study. FUM and CWH analyzed the datasets. CWH and MA performed the metagenomic assemblies. FUM and CWH performed genome analyses and phylogenetic reconstructions. FUM and AS performed NanoSIMS analyses. FUM and MM performed isotopic analyses of ^{15}N in NH_4^+ & NO_2^- . CM performed NMR and LC-MS based detection and quantification of taurine, while BG and KK performed pore water taurine quantification. FUM and M. Watzka performed bulk and TNA isotope analyses. FB performed fluorescence in situ hybridization via electron microscopy and analyzed the data. FUM and TS performed metaproteomic analyses. FUM and M. Wagner wrote the paper with support from NSW, CHW and AR. All authors discussed the results and contributed to the final paper.

FUNDING

FM and MM were supported by the ERC Advanced Grant Nitricare (294334 to MW), KK by the Wittgenstein Award of the Austrian Science Fund FWF (Z-3838), and BG by the Austrian Science Fund (FWF) Hertha-Firnberg Grant (T-1218 to BG).

COMPETING INTERESTS

The authors declare no competing interests.

ADDITIONAL INFORMATION

Supplementary information The online version contains supplementary material available at <https://doi.org/10.1038/s41396-023-01420-1>.

Correspondence and requests for materials should be addressed to Michael Wagner.

Reprints and permission information is available at <http://www.nature.com/reprints>

Publisher's note Springer Nature remains neutral with regard to jurisdictional claims in published maps and institutional affiliations.



Open Access This article is licensed under a Creative Commons Attribution 4.0 International License, which permits use, sharing, adaptation, distribution and reproduction in any medium or format, as long as you give appropriate credit to the original author(s) and the source, provide a link to the Creative Commons license, and indicate if changes were made. The images or other third party material in this article are included in the article's Creative Commons license, unless indicated otherwise in a credit line to the material. If material is not included in the article's Creative Commons license and your intended use is not permitted by statutory regulation or exceeds the permitted use, you will need to obtain permission directly from the copyright holder. To view a copy of this license, visit <http://creativecommons.org/licenses/by/4.0/>.